Aus dem

Hertie Institut für klinische Hirnforschung

Abteilung Zellbiologie Neurologischer Erkrankungen

Inaugural-Dissertation

Mechanisms of Neuronal Dysfunction in Sepsis-induced Cognitive Impairment

zur Erlangung des Doktorgrades der Medizin

der Medizinischen Fakultät der Eberhard Karls Universität zu Tübingen

vorgelegt von

Oberle, Linda Marlene

2022

Dekan: Professor Dr. B. Pichler

1. Berichterstatter: Dr. J.J. Neher
2. Berichterstatter: Prof. A. Weber

Tag der Disputation: 07.10.2021

Table of Contents

Table of Figures

Abbreviations

AD	Alzheimer's disease
ACCP	American College of Chest Physicians
BCA	bicinchoninic acid
BfR	Bundesinstitut für Risikobewertung
BSA	bovine serum albumin
BW	body weight
C	complement protein
C3	complement protein 3
C3b	activated complement protein 3
CA	Cornu Ammonis
CD11b	cluster of differentiation molecule 11b (protein)
Cd11b	cluster of differentiation molecule 11b (gene)
CLP	caecal ligation and puncture
CNS	central nervous system
CR3	Complement receptor-3
CSCC	Center for Sepsis Control and Care
CSF	cerebrospinal fluid
DG	dentate gyrus
dk	donkey
EDTA	ethylene diamine tetraacetic acid
ELISA	enzym-linked immunosorbent assay
ESICM	European Society of Intensive Care Medicine
FiO_2	p_aO_2/ fraction of inspired oxygen
Gas6	growth arrest specific gene 6
gp	guinea-pig
gt	goat
IBA1	ionized calcium-binding adapter molecule 1
ICU	Intensive care unit

ICP	intracranial brain pressure
IFN	interferon
IL	interleukin
i.p.	intraperitoneally
KC/GRO	keratinocyte chemoattractant/ human growth-regulated oncogene
LPA	lipoteichoic acid
LPS	lipopolysaccharide
Mertk	Mer receptor tyrosine kinase (protein)
Mertk	Mer receptor tyrosine kinase (gene)
MFG-E8	Milk fat globule EGF-like factor 8 (protein)
Mfge8	Milk fat globule EGF-like factor 8 (gene)
MRI	magnetic resonance imaging
NaCl	sodium chloride
NDS	Normal donkey serum
OHSCs	organotypic hippocampal slice cultures
p_aO_2	partial pressure of oxygen in blood
PBS	phosphate-buffered saline
PFA	paraformaldehyde
PS	phosphatidyl serine
PSD-95	post-synaptic density protein 95
qSOFA	quick Sequential Organ Failure Assessment
rb	rabbit
ROS	reactive oxygen species
rpm	rounds per minute
RSPy	retrosplenial area ventral part
RT	room temperature
SCCM	Society of Critical Care Medicine
SEM	standard error of the mean
SIRS	systemic inflammatory response syndrome
SOFA	Sequential Organ Failure Assessment
Tim4	T-cell immunoglobulin and mucin-domain-containing molecule-4
TLR	Toll-like receptor

TNF-α	tumor necrosis factor α
TREM2	triggering receptor expressed on myeloid cells 2
VR	vitronectin receptor

1 Abstract

Sepsis is a severe and frequent disease in modern intensive medicine. Sepsis does not only present with a mortality rate of 30% of all patients, but survivors often show long lasting cognitive deficits, loss of independency and reduced quality of life. However, the mechanisms of sepsis-induced cognitive impairments remain incompletely understood so far. To understand the mechanisms of cognitive decline in sepsis survivors, the possible involvement of the brain's primary immune cells, microglia, was investigated in this project. In particular, to investigate if and how microglia contribute to synapse loss acutely and long-term after sepsis, different phagocytosis-deficient mice strains were analyzed for synapse number and phagocytosed synapse number. To model sepsis, female mice were injected on two consecutive days with either 1.5 mg/kg body weight lipopolysaccharide (LPS), a bacterial cell wall component that induces strong inflammatory responses. At different timepoints (1 day, 3 days, 7 days or 2 months) tissue was then analysed.

Acutely after LPS-injections, quantification of phagocytic proteins showed a sharp increase in complement protein 3 in the brain. Consistently, immunohistochemical analysis revealed, that functional synapse number was strongly reduced and that the percentage of phagocytosed synapses was increased by LPS treatment. Interestingly, mice deficient in phagocytic signaling proteins (*Mfge8* $^{-}$/$^{-}$, *Cd11b*$^{-}$/$^{-}$) showed no reduction in functional synapse number and no increase in phagocytosis of functional synapses after LPS-injections. Therefore, microglial phagocytosis leads to synapse loss in a mouse model of sepsis and may contribute to long-term cognitive deficits in sepsis survivors. Inhibition of specific microglial pathways could therefore be a promising new strategy to prevent long-term cognitive deficits in sepsis survivors.

2 Introduction

Severe sepsis and septic shock are frequent diseases in modern intensive care units (ICU) and due to its high mortality rate sepsis presents crucial issue in modern medicine. Recent studies observed that patients, who survived critical illness, are at greater risk for long-term cognitive decline and show reduced cognitive performance including memory, attention and executive functions[1, 2]. However, only few studies have investigated the mechanisms of long-term cognitive impairment following critical illness, such as sepsis. These findings underline the need for further research regarding the pathogenesis of sepsis-induced long-term cognitive impairment.

2.1 Sepsis

2.1.1 History and Definition

To this day, sepsis remains a severe complication of various diseases and clinical treatments. Due to its high acute and long-term mortality, sepsis threatens the outcome of modern therapy in many disciplines e.g. abdominal surgery, transplantation medicine and oncology. This may also explain why sepsis is still not assigned to a medical discipline. Heterogeneous therapeutic strategies and definitions amongst medical disciplines are the cause of confusion and complicate the evaluation of epidemiological data [3].

Already in the 5th century BC Hippocrates marked the beginning of the history of sepsis. He described a disease, which starts 7-14 days after injury with fever, “which is caused by a matter that is fouling”. [3] Therefore, the disease was termed after the Greek origin of fouling (sepein, σηπω). Hippocrates also first raised the question whether a local injury can cause a systemic reaction and which mediators are playing a crucial role in it.

Since then, the definition of sepsis changed enormously in 1860 as Louis Pasteur and Robert Koch discovered bacteria and their pathogenic nature being the cause of different diseases including sepsis [3]. In the early 20th century Alexander Flemming discovered the first antibiotic, penicillin, which led to a revolution in medical history. Many deadly diseases caused by bacteria could now be successfully treated and even sepsis could be cured with antibiotics. [4]
However, the understanding and correspondingly the definition of sepsis kept gradually changing over the last century. As described above, in the past bacteremia was defining the pathology of sepsis. This definition is still known by the public, as sepsis is often referred to as “blood poisoning”. Even though, in only 40% of patients with severe sepsis or septic shock bacteremia can be diagnosed. Thus, studies have shown that sepsis does not only occur after systemic infections. Around 30% of sepsis cases present themselves after a sterile tissue infection, e.g. pancreatitis or cancer, demonstrating that sepsis is not restricted to a severe reaction to germs in the blood stream [5].

The basis of today’s definition of sepsis was formed 1992 during a consensus conference of the American College of Chest Physicians (ACCP) and the Society of Critical Care Medicine (SCCM) [6]. In 2003, the criteria for sepsis diagnosis were reviewed by the European Society of Intensive Care Medicine (ESICM) and sepsis was defined as a “syndrome [with] the presence of both infection and a systemic inflammatory response” [7]. To enable clinicians to diagnose sepsis fast and accurately, several diagnostic criteria (e.g. signs of infection such as fever, tachycardia; inflammatory symptoms such as leukocytosis, altered plasma C-reactive protein levels; sign of organ dysfunction such as oliguria, ileus and hemodynamic variables as hyperlactemia, hypotension) were defined [7].

Nevertheless, further research has raised the need for an updated definition due to the findings that it is not enough to solely focus on infection but that there rather is a need to include cellular and metabolic dysfunction to explain the pathogenesis of sepsis [5]. Therefore, since 2011, sepsis is referred to as ‘systemic inflammatory response syndrome’ (SIRS), which is defined as a potentially fatal

multi-organ dysfunction caused by an exaggerated immune response of the host. The definition of SIRS takes in account that sepsis-like symptoms are caused by an extensive activation of the host's immune system, which is not only triggered by bacterial infections, but also by serious diseases.

2.1.1.1 Clinical Diagnosis of sepsis

Clinically, sepsis can be grouped in three levels of severity. As sepsis is a complex and still incompletely understood clinical syndrome, different parameters and clinical tests must be assessed before diagnosis of sepsis.

Table 1: Definition criteria of sepsis according to ICD-10

Definition for diagnosis of sepsis in Germany according to ICD-10
For diagnosis, at least two blood cultures should be analyzed. 1. Negative blood culture, however patient show all four symptoms: a. Fever or hypothermia b. Tachycardia c. Tachypnea or Hypocapnia d. Leukocyctosis or Leukopenia 2. Positive blood culture and patient shows at least 2 of the symptoms listed above

To be able to diagnose sepsis, evidence or suspicion of inflammation can either be microbiologically tested by assessment of at least two blood cultures or by looking for clinical symptom of infection or SIRS (Table 1):

1. fever (≥ 38.0°C) or hypothermia (≤ 36.0°C)
2. tachycardia ≥ 90 heart beats/min
3. tachypnea ≥ 20 breaths/min or Hypocapnia (partial pressure of carbon dioxide in blood (p_aCO_2) ≤ 33 mmHg
4. leukocytosis (≥ 12 000/mm^3) or Leukopenia (≤ 4 000/mm^3)

2.1.1.2 Diagnosis of severe sepsis

For the diagnosis of severe sepsis, additional organ dysfunctions have to have been diagnosed within the last 24 hours.
Organ dysfunctions include:

1. acute encephalopathy (reduced vigilance, disorientation, delirium)

2. thrombocytopenia (thrombocytes < 100 000/µl or reduction of 30% in 24 hours without bleeding)
3. arterial hypoxemia (partial pressure of oxygen in blood (p_aO_2) < 10 kPa or p_aO_2/ fraction of inspired oxygen (FiO_2) < 33 kPa)
4. renal dysfunction (low output of urine (oliguria) < 0.5ml/ kg body weight (BW)/hour or strong increase in serum creatinine)
5. metabolic acidosis (base deficit > 5.0 mEq/l) or increase of plasma-lactate concentration 1.5-fold above upper limit

2.1.1.3 Diagnosis of septic shock

The most severe form of sepsis is septic shock. Patients with this condition suffer from the same basic symptoms as described in 2.1.1.1 but additionally show symptoms of shock. Patients are in shock if the systolic blood pressure is < 90 mmHg despite adequate volume or vasopressor (noradrenalin, adrenalin) therapy. The underlying pathomechanism is the dilatation of peripheral blood vessels causing the blood pressure to be reduced dramatically within a short time. In order to compensate, the heart rate is increased to keep up the blood circulation.

2.1.1.4 q-Sofa score

As sepsis is a life-threating disease, it is very important to minimize the elapsed time until diagnosis and antibiotic therapy is started. Therefore, a quick and easy tool was established to evaluate the probability if the patient is suffering from sepsis: quick Sequential Organ Failure Assessment (q-SOFA). The q-SOFA is derived from the more complex SOFA-score, which include also blood test results and therefore needs more time until it can be evaluated. In intensive care medicine, the q-SOFA can be assessed by simple diagnostics and saves an enormous amount of time until the first evaluation of the patient. It evaluates systolic blood pressure, breathing rate and vigilance. If two of these parameters are out of norm, patients are more likely to have worse outcomes following sepsis [8]. Although the q-SOFA has limited sensitivity as it only takes three parameters

in consideration [9], it simplifies the first evaluation and shortens the time until clinicians discuss further testing and therapy.

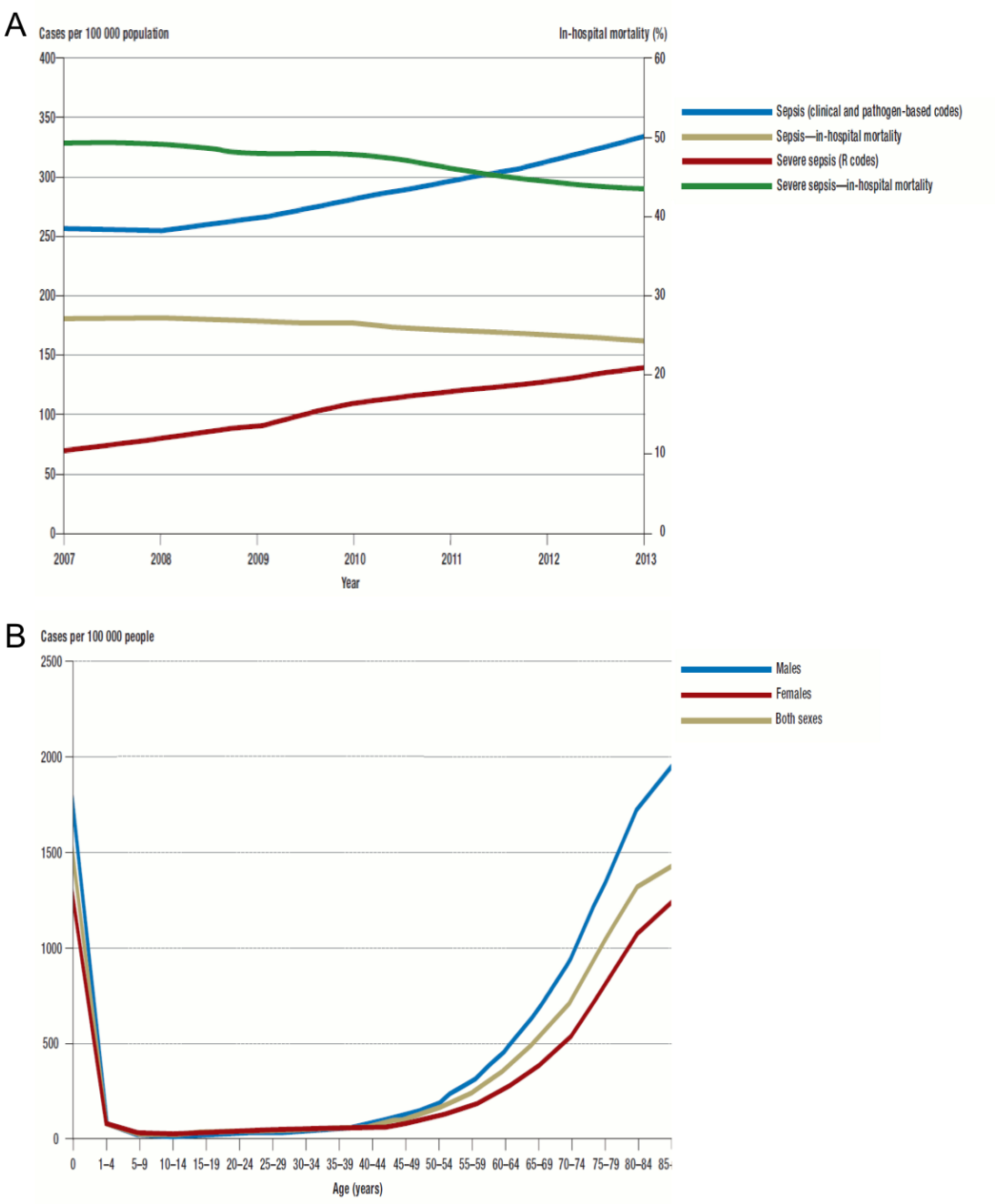

Figure 1: Epidemiology of sepsis

A) Incidence rate per 100 000 people, standardized to the German population structure in 2010, and in-hospital mortality of sepsis and severe sepsis (including septic shock) in Germany 2007-2013.
B) In-hospital incidence of sepsis per 100 000 people per year, by age group and sex, in the period 2007-2013 (clinical and pathogen-based sepsis codes).

Figure reproduced with permission from Fleischmann, C. et al. **Incidence and Mortality Rates of Sepsis: An Analysis of Hospital Episode (DRG) Statistics in Germany from 2007-2013** Dtsch. Arztebl Int 2016; 113(10): 159-66; DOI: 10.3238/arztebl.2016.0159

2.1.2 Epidemiology

Intensive care medicine has made enormous progress in the past years. Yet, incidence of long-term dysfunction after intensive care treatment could not be reduced, but instead is rising [10]. Fleischmann et al. estimate the worldwide incidence of sepsis to be 437 cases and the incidence of severe sepsis to be 270 cases per 100 000 inhabitants. [11] However, especially in low- and middle-income countries epidemiological data is missing and rates are likely to be higher.

Between 2007 to 2013, the German center for sepsis control and care (CSCC), associated with the university hospital Jena, has analyzed epidemiological data of sepsis diagnosis in German hospitals using nationwide case-related hospital DRG statistics. According to the study, incidence of sepsis rose to 473 cases per 100 000 inhabitants including all forms of sepsis, resulting in a total number of approximately 400 000 sepsis patients in Germany per year [12]. Furthermore, the study revealed that the annual incidence rate rises gradually after the age of 40, after a first peak during neonatal age, reaching a second peak at age 85 and above with annual numbers of 1 434 patients per 100 000 inhabitants. Therefore, sepsis is pre-dominantly a disease of the older patient with approximately two thirds of patients aged over 65-years.

The in-hospital mortality rate of sepsis and severe sepsis declined over the years 2007 to 2013 from around 27% and 50% to 25% and 44%, respectively. However, mortality is strongly age dependent. Whereas in-hospital mortality of 20-year-old patients is approximately 5%, it rises steadily to over 35% for 85-year-old patients [12] showing that especially elderly people are at risk to develop sepsis and to succumb to it. Hence, sepsis is in third place among the most frequent causes of death in Germany.

These data show, that sepsis is a frequent disease worldwide with a high risk of death and most prominently affecting newborn and elderly people and causing the death of one third to one half of these patients (Figure 1).

2.1.3 Hospital-related cost of sepsis

Considering the increasing success in treating life-threatening diseases and the aging of the society, sepsis and other critical illnesses may give rise to a global health problem and considerable annual costs [13, 14].

Due to the intensive and long-term therapy needed in cases of sepsis, treatment sums up to extremely high costs. The estimated hospital-related costs vary greatly between different studies. The average cost per patient in first world countries varies between $20 000 to $30 000 [15-17], amounting to annual costs of $10-20 billion in the US.

However, the direct medical cost of sepsis is not the only financial burden, that society has to face regarding the treatment of sepsis. Since many patients develop long-term impairments and disabilities, less than 50% of ICU survivors will return to work [13, 18]. In Germany, the productivity loss due to permanent morbidity is estimated to range between 450-1000 Mio EUR (upper and lower end of incidence) and due to temporary morbidity between 150-300 Mio EUR per year. Premature death causes an economic burden of 2 000-4 000 Mio EUR per year in Germany [19] (Table 2).

Table 2: Financial burden of severe sepsis in Germany

Burden of Illness of severe sepsis			
Total costs of severe sepsis in Germany (in Mio EUR)			
Direct costs			
Total cost	**1 000**	**–**	**2 200**
Indirect costs			
Productivity loss due to temporary morbidity	150	–	330
Productivity loss due to permanent morbidity	450	–	1.000
Productivity loss due to mortality	2 000	–	5 600
Total cost	**2 600**	**–**	**6 930**
Burden of Illness	**3 600**	–	**9 130**

Adapted from: Schmid et al, 2002

2.1.4 Cognitive decline after Sepsis

Cognitive decline is a frequent and severe complication of sepsis and affects approximately 60% of all patients [20, 21]. It is also associated with an increase of mortality and manifests as reduced cognitive performance, e.g. memory and executive functions [22-24]. Especially elderly people have worse outcome after experiencing critical illness like sepsis. As more than half of all ICU patients are older than 65-years [2], most of ICU treated sepsis patients experience cognitive decline [24], resulting in loss of independence and reduced quality of life, often associated with institutionalization, hospitalization and residential care [25]. Less than 50 % of patients will ever return to normal life and work [13, 14], thus leading to high health care costs after intensive care treatment (section 2.1.3).

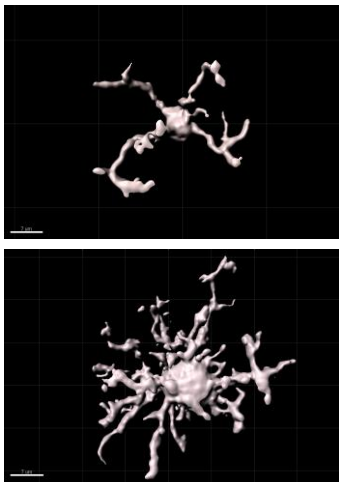

Figure 2: Morphology of microglia

A. Resting microglia: round and small cell body with thin, ramified processes. IBA1 positive cell, reconstituted using Imaris (Bitplane), of a PBS-injected wildtype animal, 1 day post injection.
B. Activated microglia: large cell body and short processes. IBA1 positive cell, reconstituted using Imaris (Bitplane), of an LPS-injected wildtype animal, 1 day post injection.

While the pathophysiology that leads to cognitive decline remains incompletely understood, magnetic resonance imaging (MRI) studies of septic patients reported white matter loss, leukoencephalopathy, ischemic stroke [26], as well as brain atrophy in the frontal cortex and hippocampus [27, 28]. Accordingly, brain atrophy was found by a recent post-mortem study of fatal sepsis cases [29]. Interestingly, the brain's resident macrophages, microglia, have been found to be proliferating and activated [30] implicating an association between peripheral inflammation and microglial activation and response, which could be contributing to cognitive decline after sepsis.

2.2 Primary effector cells in the brain

In order to process the complex information our brain receives every second, billions of neurons form complex networks. However, other cell types are also

needed for the proper function of the central nervous system (CNS). Neuroglial cells - microglia, astrocytes and oligodendrocytes - have been found to constitute around one third to two thirds of all brain cells [31]. As astrocytes are the most common neuroglia cells, the vast functions of these cells in healthy brains are fairly well described. In short, their function is to maintain water and ion homeostasis in the brain and their processes play a critical role in stabilization of the blood-brain barrier [32]. The second type of neuroglial cells, oligodendrocytes, has been found to build up the myelin sheaths of neuronal axons, which is necessary for the fast saltatory conduction of action potentials [32]. Last but not least, microglia cells are a type of self-renewing [33, 34], tissue-resident macrophage presenting the predominant type of immune cell in the CNS. Microglia represent 10-15% of all cells in the brain and spinal cord and are found throughout in the CNS [35, 36]. They maintain tissue homeostasis by continuously examining their microenvironment and phagocytosing dead or dying neurons or potentially harmful extracellular components. [37] In order to fulfil their vast functions, they undergo a variety of structural changes depending on their activation state. In their resting state, microglia cell bodies are round, their processes are long, covering a large area and as a cell population, they scan the entire brain every few hours. After activation, their form changes to a larger soma and shortened processes [38] (Figure 2).

2.3 Physiological role of phagocytosis in the brain

Phagocytosis plays a critical role in maintaining homeostasis and preventing diseases in the body and the brain. One of the most important functions of phagocytosis is the rapid clearance of apoptotic cells [39]. This process is necessary to prevent the release of intracellular components from dying cells and thereby prevents autoimmunity [40]. This is evidenced by the finding that phagocytosis-deficient mouse models often develop autoimmune phenotypes, likely due to the inadequate clearance of apoptotic cells in the body and the release of autoantigens [41, 42].

The specialized cells for phagocytosis in the brain are microglia. For example, microglial phagocytosis of age-related myelin debris is impaired in the aged brain, leading to accumulation of myelin debris in the CNS and contributing to aged-related cognitive decline [43, 44]. Similarly, phagocytic processes are also likely to contribute to the removal of amyloid plaques in Alzheimer's disease [45] (AD) and genetic studies have shown that mutations in microglia-related genes are risk factors for AD [46, 47]. Therefore, failure or dysfunction in the phagocytosis and/or degradation of plaques by microglia may accelerate Alzheimer's disease [48]. Moreover, microglial dysfunction is not only discussed in AD pathology but in many proteopathic diseases like Creutzfeld-Jakob-Disease and Parkinson's Disease [49, 50]. Of note, microglia do not only phagocytose dying cells and amyloid aggregates but also neuronal synapses. This so-called synaptic pruning will be discussed in section 2.3.2.

2.3.1 Mechanism of microglial phagocytosis

After activation, microglia phagocytose potentially harmful components in a receptor-mediated three step process including "find-me", "eat-me" and "digest-me" signals. The release of special chemotactic signals induces the attraction of nearby microglia cells. On the cell-surface, dying neurons expose "eat-me" signals, which mediate cell attachment and provoke the cell to be engulfed, transported to the lysosomes and finally degraded by microglia [51].

The probably best known and most intensely studied eat-me-signal is phosphatidyl serine (PS). PS is usually found in the inner leaflet of the cell's phospholipid bilayer membrane and is therefore normally hidden from the surrounding cells [38-40].

There are several described reasons for PS exposure: i) plasma membrane rupture due to necrosis, ii) inhibition of aminophospholipid translocase, which swaps PS from the outer to the inner membrane, iii) ATP depletion [52] or oxidative stress, which limit the activity of the aminophospholipid translocase [53], iv) calcium elevation activates phospholipid scramblase, leading to PS exposure [54].

Interestingly, it has been shown, that in response to cellular stress which is not sufficient to induce apoptosis, so-called stressed-but-viable neurons can reversibly externalize PS [55, 56]. In the presence of microglia cells, such neurons which externalize PS are engulfed, whereas in the absence of microglia or by blocking the recognition of PS by microglia cells, these neurons survive and re-internalize PS [55-57].

2.3.1.1 Phosphatidylserine binding receptors and opsonins

PS is recognized by microglia via different membrane receptors depending on the activation state of the cells. For example resting microglia cells recognize PS via T-cell immunoglobulin and mucin-domain-containing molecule-4 (Tim4) [58, 59], whereas activated microglia cells produce the key PS-binding molecule Milk fat globule EGF-like factor 8 (MFG-E8), also known as lactadherin or SED1 [60] (Figure 3).

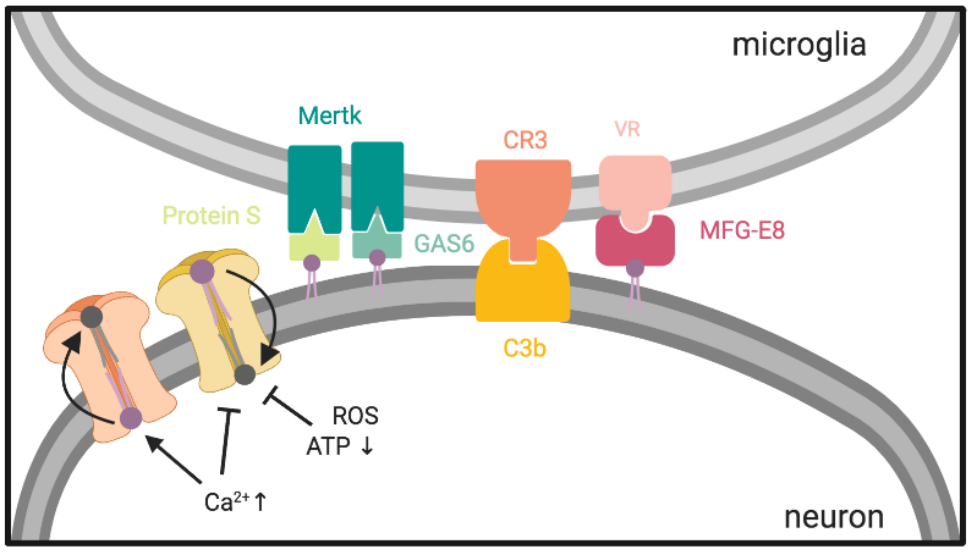

Figure 3: Signaling pathways implicated in phagocytosis of neurons

Microglia are important to maintain the homeostasis in the brain by continuous examination of their microenvironment and phagocytosing dead or dying neurons or potentially harmful extracellular components. Different pathways are known to contribute to the cytoskeleton rearrangements and phagocytosis. Dead or dying neurons expose phosphatidylserine (PS), either by activation of phospholipid scramblase (orange) or by inhibition of aminophospholipid translocase (yellow). Microglia recognize exposed PS via different receptors, e.g vitronectin receptor (VR) or Mer receptor tyrosine kinase (Mertk) and opsonins like Milk fat globule EGF-like factor 8 (MFG-E8), protein S or growth arrest specific gene 6 (Gas6). Activated complement protein 3 (C3b) and its receptor, complement receptor-3 (CR3) are especially important for phagocytosing neuronal structures like synapses.

2.3.1.1.1 Milk fat globule EGF-like factor 8

MFG-E8 is a membrane-associated glycoprotein and expressed ubiquitously in almost all organs in mice, humans and other mammals [61]. In the brain MFG-E8 is produced not only by microglia but also by astrocytes. Previous studies showed, that MFG-E8 plays an important role in tissue remodeling [62, 63] and enhances the phagocytosis of apoptotic cells by acting as a bridging molecule between apoptotic cells and phagocytes [60] via vitronectin receptor (VR), an $\alpha_v\beta_{3/5}$ integrin [56]. Interestingly, it could be demonstrated, that microglial phagocytosis was inhibited after blocking either MFG-E8 directly or inhibiting binding to the VR using antibodies [64].

2.3.1.1.2 Mer receptor tyrosine kinase

In addition to the role of the opsonin MFG-E8 in apoptotic cells by microglia, the Mer receptor tyrosine kinase (Mertk), a member of the TAM receptor protein tyrosine kinases, also mediates apoptotic cell uptake. Mertk is broadly expressed in vascular, immune, nervous and reproductive systems [65]. Moreover, studies have revealed that Mertk recognize PS indirectly through bridging molecules like growth arrest specific gene 6 (Gas6) or Protein S [65-67]. Furthermore, Mertk deficient mice were unable to clear apoptotic cells and membranes adequately. This state could be reversed in chimeric mice after bone-marrow transplantation from wildtype mice [67].

2.3.1.1.3 Cluster of differentiation molecule 11b

The most studied protein for phagocytic removal of synapses is Cluster of differentiation molecule 11b (CD11b). CD11b is the α-chain of the integrin receptor CD11b/CD18, which is also known as Mac-1 and complement receptor-3 (CR3), and is found on the surface of microglia [68] and other innate immune cells [69, 70].

In the past years, it has been found that CD11b/CR3 is important for vast functions of the innate immune system like migration of leukocytes [71] and

phagocytosis [72, 73]. As complement protein 3 is one of its ligands, CD11b receptor is a key molecule in synaptic pruning by microglia.

2.3.2 Microglial synaptic pruning

In healthy brains inactive synapses are eliminated by microglia in a complement-dependent manner [74]. The complement cascade is normally initiated by activation of complement protein (C) 1q which than activates C2 and C4 in order to cleave C3 into C3a and C3b, its active form. In the brain, CR3 is expressed by microglia cells which recognize inactive synapses through C3b/CR3-signaling, resulting in engulfment of these synapses [74]. Interestingly, it has been found that synaptic pruning is unaffected by lack of C1q, indicating an alternative pathway for C3 activation [75].

However, recent evidence indicates that synaptic pruning does not only occur during development of neuronal circuits but also throughout life in order to remove dying neurons and weak synapses. In particular, it has been found that activation of CR3 results in phagocytosis of PS exposing neuronal structures [74, 76], supporting the idea that dysregulation in this process might contribute to disease progression. Recently, a mouse study has shown that neuronal loss after peripheral inflammation induced by repeated LPS-injection over 4 days could be prevented in C3 deficient mice [72]. This indicates that complement-mediated phagocytosis may contribute to neuronal degeneration and cognitive impairment after inflammation.

2.4 Detrimental effects of microglial phagocytosis

In the past, microglial phagocytosis was considered to be a beneficial process as it was found to be crucial for maintainance of brain homeostasis [51]. However, recently it has been found that during brain ischemia and consecutively inflammation, phagocytosis can be detrimental and execute the death of stress-but-viable neurons [55]. After activation of glial-neuronal cultures using lipoteichoic acid (LPA) or LPS, both bacterial cell wall components, activated microglia produce reactive oxygen and nitrogen species which provokes PS exposure on

neurons [77]. Additionally, activation of microglial cells leads to an increased release of MFG-E8 which induces phagocytosis by acting as an opsonin between exposed PS and the microglial vitronectin receptor [56]. Furthermore, in a rodent model of focal ischemia, phagocytic proteins like MFG-E8 or Mertk were upregulated. Mice deficient for MFG-E8 or Mertk survived with a better sensorimotor outcome and less neuronal death in comparison to wildtype littermates [57]. Of note, arterial hypoxemia and hypotension are defining criteria for sepsis shock [78] indicating that reduced cranial perfusion and low oxygen blood levels may be contributing to septic encephalopathy and cognitive decline.

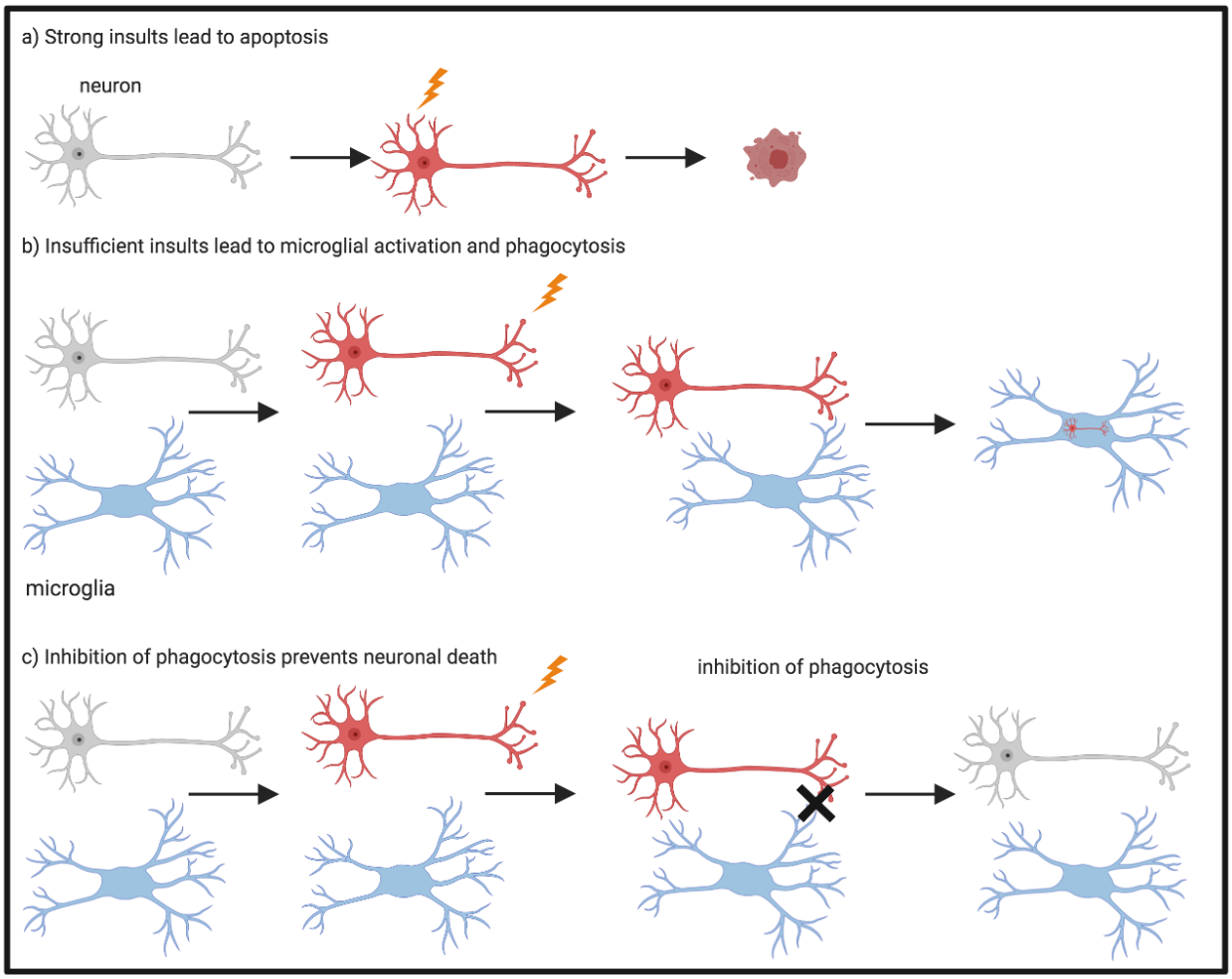

Figure 4: Phagocytosis of stressed-but-viable neurons

Hypoxemia, stress and inflammation is known to induce “eat-me-signals” like PS to be exposed by neurons. (a) If the external stress is sufficient, neurons will undergo apoptosis. (b) However, if the insult is insufficient to induce apoptosis, PS-exposure activates microglia cell to phagocytose neurons and synapses. (c) If phagocytosis Is inhibited, these so called “stressed-but-viable neurons” will re-internalize the exposed “eat-me-signals” and survive.

2.5 Animal models of sepsis

In order to investigate the pathology of sepsis, three main models have been established in the last years: i) administration of a viable pathogen, ii) interrupting the host endogenous protective barrier, for example by caecal ligation and puncture, iii) intraperitoneal (i.p.) administration of endotoxin (i.e. lipopolysaccharide (LPS)). [79]

These different animal models of sepsis have advantages and deficiencies. Physiologically, sepsis is often caused by mixed cultures of vital pathogens and therefore, the administration of viable bacteria and caecal ligation and puncture (CLP) are more suitable methods to mimic the physiological course of the disease. [79] However, a great benefit of LPS injection models is the reproducibility and standardization. By using a specific dose of LPS, similar physiological changes can be consistently induced in many animals. [79] As a result, inter-individual differences are reduced and differences due to experimental manipulation will more readily be apparent. Especially in CLP, different intensity of immune stimulation can be expected, which might influence the outcome of the experiments. Furthermore, the danger of viable pathogens to the animals can lead to unpredictable death rates, thus a greater number of animals have to be treated. For these reasons, the use of LPS injections is often the model of choice. LPS is a gram-negative cell wall component and activates Toll-like receptor 4 (TLR4), inducing tumor necrosis factor α (TNF-α), Interleukin (IL)-1β, IL-1α or IL-6 production. In patients, these pro-inflammatory cytokines lead to an alteration in brain function, inducing acute sickness behavior being defined by lethargy, decreased motor activity and reduced food intake [80]. A similar behavior can be observed in rodents after intraperitoneal LPS-injections [81].

Although LPS is not able to mimic the heterogenous effects and complexity of sepsis observed in humans, intraperitoneal LPS-injection has been found to induce affective alterations like depression and anxiety as well as cognitive impairments [79, 82]. Furthermore, neuroinflammatory and microglial activation has been found to be elevated [83]. Additionally, neuronal loss was described to be mostly affecting the hippocampus after LPS-injections [84-86]. Therefore, in this

study i.p. LPS-injected mice were used as a model for sepsis to investigate the detrimental effects of sepsis on the brain.

2.6 Aim of the study

To further understand the detrimental effects of sepsis on the brain, this study investigated if microglial phagocytosis in general and which specific phagocytic signaling contributes to synapse loss by manipulating different phagocytic pathways. To this end, we quantified synapse number and phagocytosed synapse number in wildtype and phagocytic protein deficient mouse strains *(Mfge8, Cd11b)* at different timepoints (1 day, 3 days or 2 months) after two consecutive i.p. LPS or phosphate-buffered saline (PBS) injections using immunohistochemistry. Furthermore, we quantified brain concentration of phagocytic opsonin using enzym-linked immunosorbent assay (ELISA). By increasing the understanding of the detrimental effects of sepsis to the brain, targeted therapy to prevent cognitive deficits in survivors of sepsis could be developed in the future.

3 Materials and methods

3.1 Mice

To investigate the mechanism of sepsis-induced neurodegeneration, several transgenic mouse strains were used. The animals were raised, treated and perfused by the group of Dr. med. Julius Emmrich at the Bundesinstitut für Risikobewertung (BfR), Berlin. The mice were maintained under specific pathogen-free conditions at and with free access to standard food and water. Of note, only female mice were used for the study. To exclude bias of genotype-mediated behavior to the testing, wildtype and knockout female mice were housed together. All experiments were performed in accordance with the veterinary office regulations approved by the Ethical Commission for animal experimentation of the Landesamt für Gesundheit und Soziales in Berlin, Germany (G239/15).

3.1.1 *Mfge8* knockout

The mice were raised on a C57BL/6J background. The functional knockout of *Mfge8* was generated by replacing the C2 domain of *Mfge8* with a transmembrane-β-geo reporter gene, retaining MFG-E8 inside the membrane and inhibiting the release of MFG-E8 leading to rapid degradation of the protein [63]. The mice were generously provided by C. Théry, INSERM 932, France.

3.1.2 *CD11b* knockout

The mice were raised on a C57BL/6J background. These mice are homozygous for the I*tgam*^{tm1Myd} targeted mutation (B6.129S4-*Itgam*^{tm1Myd}/J, The Jackson Laboratory). These mice lack the integrin α-M-gene, which encodes CD11b, one subunit of the CR3 receptor. The mice show no physical or behavioral abnormalities, but homozygous mutants show deficiency in neutrophil spreading and phagocytosis [87].

3.1.3 *Mertk* knockout

The mice were raised on a C57BL/6J and 129S1/SvImJ background. These mice are homozygous for the *Mertk* targeted mutation 1 (tm1GrL; Jackson Laboratory). The gene was knocked out by replacing a part of the essential kinase domain with a neomycin selected cassette. The animals show no gross physical or behavioral abnormalities [88].

For *Mfge8 and Cd11b* $^{-}$/-, C57BL/6J or wildtype offspring from het x het breeding was used as controls. For *Mertk* $^{-}$/-, only wildtype offspring was used. Every mouse was genotyped by Eurofins using ear biopsy.

3.2 Number of Animals

Table 3: Number of animals

			C3 - ELISA	MFG-E8 - ELISA	Mesoscale cytokine	Cresyl violet staining	IBA1, Bassoon, PSD-95 staining
Mfge8 $^{+}$/$_{+}$	1d	LPS	7	5	0	0	6
		PBS	2	2	0	0	2
	3d	LPS	7	5	0	0	6
		PBS	1	3	0	0	1
	7d	LPS	7	5	0	0	6
		PBS	2	2	0	0	2
	2 months	LPS	7	5	5	0	6
		PBS	2	2	5	0	6
Mfge8 $^{-}$/-	1d	LPS	7	0	0	0	6
		PBS	2	0	0	0	2
	3d	LPS	6	0	0	0	4
		PBS	2	0	0	0	2
	7d	LPS	5	0	0	0	5
		PBS	2	0	0	0	2
	2 months	LPS	8	0	3	0	5
		PBS	2	0	3	0	5
Cd11b $^{+}$/$_{+}$	1d	LPS	7	3	0	0	5
		PBS	2	2	0	0	2
	3d	LPS	6	3	0	0	5
		PBS	2	2	0	0	2

	7d	LPS	7	3	0	0	0
		PBS	2	2	0	0	0
	2 months	LPS	7	3	5	0	5
		PBS	2	2	5	0	4
Cd11b $^{-/-}$	1d	LPS	6	5	0	0	7
		PBS	3	2	0	0	2
	3d	LPS	5	4	0	0	6
		PBS	2	2	0	0	3
	7d	LPS	5	5	0	0	0
		PBS	2	2	0	0	0
	2 months	LPS	7	5	3	0	5
		PBS	2	2	3	0	5
Mertk $^{+/+}$	1d	LPS	7	5	0	0	0
		PBS	2	2	0	0	0
	3d	LPS	7	5	0	0	0
		PBS	2	2	0	0	0
	7d	LPS	7	5	0	0	0
		PBS	2	2	0	0	0
	2 months	LPS	7	5	5	0	0
		PBS	2	2	5	0	0
Mertk $^{-/-}$	1d	LPS	8	5	0	0	0
		PBS	2	3	0	0	0
	3d	LPS	7	5	0	0	0
		PBS	2	2	0	0	0
	7d	LPS	7	4	0	0	0
		PBS	2	2	0	0	0
	2 months	LPS	9	5	3	0	0
		PBS	2	2	3	0	0
C57BL/6J	1d	LPS	0	0	0	5	0
		PBS	0	0	0	2	0
	3d	LPS	0	0	0	5	0
		PBS	0	0	0	2	0
	7d	LPS	0	0	0	5	0
		PBS	0	0	0	2	0
	2 months	LPS	0	0	0	5	0
		PBS	0	0	0	2	0

Number of animals per timepoint and genotype used for the indicated analyses.

3.3 Peripheral Immune Stimulation

At the age of eight to twelve weeks, female mice were randomly assigned to treatment groups and either injected intraperitoneally (i.p.) with 1.5 mg/kg body weight (BW) LPS (from Salmonella enterica serotype, Sigma-Aldrich) or with PBS (Lonza) on two consecutive days [89].

3.4 Tissue collection

The animals were euthanized either after 1 day, 3 days, 7 days or 2 months and transcardially perfused with ice-cold PBS (Lonza) through the left ventricle. The brain was removed and separated sagitally. One half of the brain was directly frozen on dry ice, the other hemisphere was fixed in 4% paraformaldehyde (PFA, Electran) (see 3.6.1). Serum was collected by centrifugation of venous blood for 10 minutes at 33 000 rounds per minute (rpm) at 22 °C in vacuette tube (greiner bio-one).

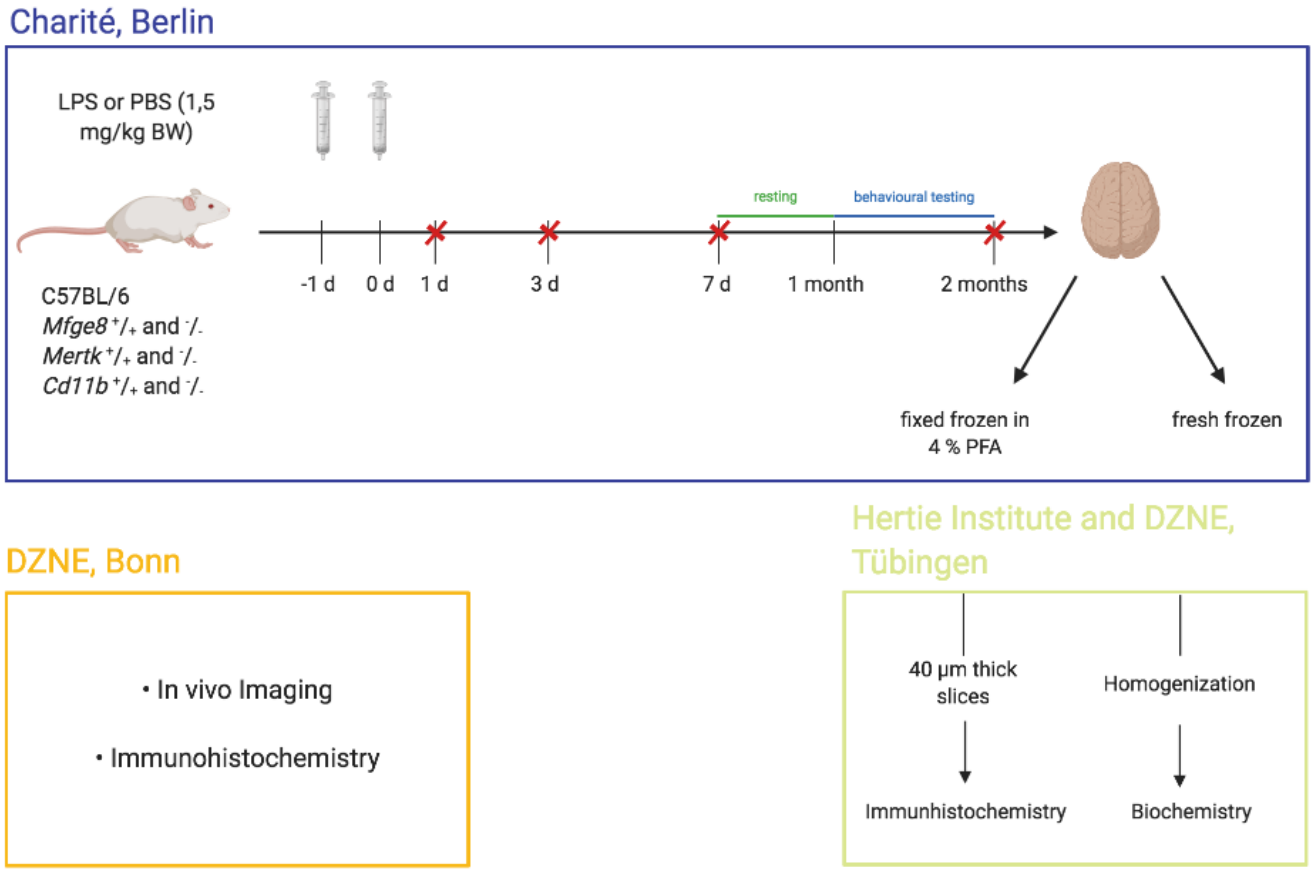

Figure 5: Overview of complete project design (including contributions of collaborators)

At the age of 3 months, female mice of different genotypes (*C57BL/6, Mfge8, Cd11b* and *Mertk* wildtype ($^{+}/_{+}$) and knockout ($^{-}/_{-}$)) were i.p. injected on two consecutive days either with LPS or PBS and either sacrificed after 1 day, 3 days, 7 days or 2 months post-injection. One half of the brain was directly fresh frozen, the other half was fixed in 4% PFA. The fresh frozen brain was homogenized and used for biochemistry (ELISA), whereas the fixed brain was cut into 40 µm thick slices and used for immunohistochemistry.

3.5 Biochemical Analysis

3.5.1 Brain homogenization

After preparation, one hemisphere was directly fresh frozen on dry ice. This half of the brain was stored at -80°C until it was homogenized in homogenization buffer (50mM Tris pH8, 150 mM NaCl and 5 mM EDTA). Right before use, a protease inhibitor (Merck, complete™ Mini EDTA-free Protease Inhibitor Cocktail) was added. The brain was weighed and homogenization buffer was added to achieve 20% brain homogenates. The brains were then homogenized using a Precellys® lysing kit (Peqlab Biotechnology GmbH) at 5500 rpm for 2 times 10 seconds with 10 seconds break in between. After aliquoting, the samples were stored at -80°C for further biochemical analysis.

3.5.2 Enzym-linked Immunosorbent Assay (ELISA)

3.5.2.1 Mouse Complement Protein 3

In order to investigate the level of Complement Protein 3 (C3) in brain homogenates, mouse Complement C3 ELISA Kit (Abcam, product number ab157711) was carried out following manufacturer's instructions. According to the manufacturer's information, the ELISA Kit recognizes the complete C3 protein as well as C3a and C3b. To further homogenize the brain suspension, homogenate was aspirated 2-3 times in 1.0 ml subcutaneous syringe (BD Plastipak Sub-Q) before using the tissue for the ELISA. Brain homogenates were diluted 1:5 in diluent buffer of the kit. Measurements were performed on FLUOstar Omega (BMG Labtech) and results were normalized to brain protein concentration, analyzed using bicinchoninic acid (BCA) assay (section 3.5.4). For analysis, samples of PBS-treated animals from different timepoints (1d, 3d, 7d and 2 months) were used to compensate for potential batch effects. However, measures were found to be consistent between different PBS groups. Based on previous experiments, measurements were expected to be highly reproducible between technical replicates, and therefore, technical replicates were omitted in favor of increasing the number of biological replicates.

3.5.2.2 Mouse MFG-E8 ELISA

The mouse MFG-E8 ELISA (Quantikine® ELISA, R&D Systems, product number MFG-E80) was carried out following the manufacturer's instruction. The samples were diluted to 1:10 in diluent buffer. By retracting the homogenates several times into a 1.0 ml subcutaneous syringe (BD Plastipak Sub-Q), the samples were further homogenized before applying the samples onto the ELISA. Measurements were performed on FLUOstar Omega (BMG labtech) and results were normalized to brain protein concentration, analyzed using BCA (section 3.5.4). For analysis, samples of PBS-treated animals from different timepoints (1d, 3d, 7d and 2 months) were used to compensate for potential batch effects. However, measures were found to be consistent between different PBS groups. Based on previous experiments, measurements were expected to be highly reproducible between technical replicates, and therefore, technical replicates were omitted in favor of increasing the number of biological replicates.

3.5.3 Quantification of cytokine levels in brain tissue

To analyze brain cytokine levels, proinflammatory panel 1 mouse kit (Mesoscale Discovery, catalog number: K15048D) was performed following the alternate protocol 1 of the company. Thus, the samples were incubated not only for two hours but overnight at 4°C. The results were normalized to brain protein concentration, analyzed using BCA (section 3.5.4). Based on previous experiments, measurements were expected to be highly reproducible between technical replicates, and therefore, technical replicates were omitted in favor of increasing the number of biological replicates.

3.5.4 Microplate bicinchoninic acid (BCA) assay

For total protein concentration analysis, bovine serum albumin (BSA, ThermoScientific) was diluted with water to create protein standard. Brain homogenates were diluted 1:25 in water. 25 µl of diluted brain homogenates were pipetted on ice in a 96-well plate. Shortly before use, BCA working reagent A (Pierce) was mixed with reagent B (Pierce) in 50:1 ratio. 200 µl of mixed BCA working reagent were then quickly added to each well. After incubation at 37°C

for 30 minutes, intensity was measured at 562 nm with reference values at 750 nm in FLUOstar Omega (BMG labtech). The final concentrations were calculated based on the blank corrected standard values minus 750nm reference values using Microsoft® Excel Version 16.16.13. The results were used to normalize C3, MFG-E8- and cytokine brain concentrations.

3.6 Immunohistological analysis

3.6.1 Brain sectioning

For immunohistochemistry, one brain hemisphere was fixed in 4% paraformaldehyde (PFA, Electran) in PBS (Lonza) for 24 hour and cryoprotected in 30% sucrose (Roth) in PBS for another two days. Afterwards, the brain was frozen in 2-methylbutane (VWR) and stored at -80°C until the tissue was cut in 40 µm coronal sections with a freezing-sliding microtom (Leica or SLEE). Sections were stored in tissue protection solution (250 ml Ethylene glycol (Ensure), 300 ml glycerol (PanReac AppliChem), 450 ml PBS) at -20°C.
Tissue that was damaged due to insufficient cryoprotection or cooling during transport was excluded by a blinded experimenter from further analysis. Mostly, tissue of the 7 days post-injection group was affected. Therefore, only good quality tissue of animals at 1 day, 3 days and 2 months post injections were used for immunohistological analysis. No more animals could be treated to increase animal number.

3.6.2 Cresyl violet staining

After the slices were washed three times for 10 minutes in PBS (Lonza), all sections from one well were mounted on slides (Microscope KP plus Printer Slides (26 x 76 x 1 mm) and dried for at least half an hour at 37°C. Cresyl violet stock solution (0.1 g Cresyl violet (Sigma Aldrich) was mixed in 100ml H_2O and heated to dissolve and filtered. Then it was pre-heated at 60°C. Shortly before use, 5 drops of 10% glacial acetic acid (Emsure) were added per 30 ml cresyl violet solution. Afterwards, sections were rehydrated in PBS and incubated with cresyl violet for 5 minutes. Then, slices were shortly put in 70% and 96% ethanol

(PanReac AppliChem) and dehydrated in 96% ethanol for 3 minutes, in 100% ethanol two times for 3-5 minutes each and in Xylol (PanReac AppliChem) three times for 3-5 minutes each. Afterwards, slices were covered with Pertex (Medite) and coverslipped.

3.6.2.1 Quantification of Brain Volume

Per animal 12-16 sections were analyzed, reflecting a 12th of the total sectioned brain. For high-throughput mode, images were automatically digitized by Zeiss AxioScan.Z1 at 10x magnification (Zeiss Plan Apochromatx10/0.45NA).
The images were then individually opened with ImageJ Software (Version 2.0.0). Each section was analyzed for the area of Cortex, total hemisphere, total hippocampus, Cornu Ammonis (CA) 1 and CA3 region and ventricles (Figure 8). The olfactory bulb and cerebellum were not included in the analysis. The number of pixels of every section was summed up for each individual animal and the sum was converted into cubic millimeters for comparison.

3.6.3 PSD95, IBA1 and Bassoon co-staining

Blocking solution	20% normal donkey serum (NDS, Fisher Scientific) in PBS (Lonza)
Primary antibody solution	rabbit-(rb)-anti-PSD95 (1:750, Invitrogen) guinea-pig-(gp)-anti-Bassoon (1:500, Synaptic Systems) goat-(gt)-anti-IBA1 (1:500, Novusbio) in 10% NDS and 0.3% Trition X-100 (Sigma Aldrich) in PBS
Secondary antibody solution	donkey-(dk)-anti-rb Alexa488 (1:250, Dianova) dk-anti-goat Alexa568 (1:250, Invitrogen) dk-anti-gp Alexa647 (1:250, Dianova) in 10% NDS and 0.3% Trition X-100 in PBS

Three hippocampal sections of each mouse were randomly chosen and immunostained for pre- (Bassoon) and postsynaptic (postsynaptic density protein 95 (PSD-95)) proteins and ionized calcium-binding adapter molecule 1 (IBA1), a protein specifically and strongly expressed in microglia cells.

After washing 3 times for 10 minutes with PBS, the sections were incubated in blocking solution for 60 minutes at room temperature (RT) on a shaker, followed by incubation in primary antibody solution at 4°C overnight on a shaker.
The next day, the sections were again washed 3 times for 10 minutes and incubated for 3h at RT in darkness in secondary antibody solution. After washing, the sections were mounted on slides (Microscope KP plus Printer Slides, 26 x 76 x 1 mm) and covered with coverslips using DAKO Fluorescent Media.

3.6.3.1 Quantification of synapse number

The animal identifiers were blinded before recording the images using a Confocal Microscope (TCS SP8, Leica; objective: HC PL APO CS2 40x, NA 1.3). Two z-stacks of the retrosplenial area ventral part (RSPv, now only referred to as cortex) of the cortex and hippocampal Cornu Ammonis 1 (CA1) region of each slide were recorded using the following settings: z-steps 32, 0.33 µm interval, line average 2, resolution 1024 x 1024, Zoom 1, Pinhole 1AU.
The images were then analyzed using ImageJ (Version 2.0.0) Plug-in Puncta Analyzer (written by Bary Wark)[90] to quantify the total pre-, post- and functional synapse number, being defined as colocalization of pre- and postsynaptic proteins. Before analyzing, the contrast was automatically adjusted. The Bassoon and PSD95 channels were merged leaving out the IBA1 channel. Afterwards 4 maximal intensity projects were created and transformed to RGB pictures. Each picture was analyzed with individual thresholds within the second range of contrast, rolling ball radius of 50 and minimum pixel size of 4.

3.6.3.2 Quantification of phagocytosed synapse number

The images were again analyzed using Imaris software (Bitplane, Version 9.3.1) to quantify the number of functional synapses inside IBA1 positive microglial cells.
First, a virtual surface of the microglia was generated using the preset settings (surface detail 0.361) and adapting the threshold individually for each picture to achieve full cell reconstruction. Afterwards three microglia were randomly selected and the Bassoon and PSD95 channels were masked using the IBA1

surface, creating a new channel of pre- and postsynapses, which are inside IBA1 positive cells. Then, colocalization of the masked Bassoon and PSD95 channels was calculated using the colocalization and threshold adaption tool of Imaris. Finally, surfaces of the colocalized puncta were automatically created using the following settings: detail surface 0.04; the threshold was calculated automatically by Imaris. The volume and number of the phagocytosed synapses were calculated by Imaris.

3.7 Statistics

Statistical analysis was performed using Prism 9 software. Data were tested for statistical outliers (Grubbs's Test, α=0,05). Before statistical analysis, data was tested for normality using Shapiro-Wilk normality test. For normally distributed data, one-way ANOVA or in case of non-normally distributed data, the non-parametric data Kruskal-Wallis-Test were used, followed by post-hoc-testing with Tukey's multiple comparison test or Dunn's multiple comparison test, respectively. For grouped analysis, two-way ANOVA with post-hoc testing with Dunnett's multiple comparisons test or Šídák's multiple comparisons test was performed. Dunnett's multiple comparisons test was chosen, if comparisons were only against the control group (PBS), Šídák's multiple comparisons test was used, if all groups were compared against each other (PBS, LSP 1dpi, 3dpi, 7dpi and 2months). Further information can be found in the figure legends.

4 Results

4.1 Peripheral LPS-injections induce inflammation in the brain

4.1.1 Complement protein 3 concentration rises acutely after LPS-injections

To investigate whether peripheral LPS-injections induce an innate immune reaction in the brain, complement protein 3 concentration was quantified in brain homogenates by ELISA. LPS is known to strongly induce the complement cascade [91], and accordingly, C3 levels were significantly increased 1 day (58.3 ± 7.5 ng/mg total protein) after LPS-injections in comparison to PBS-injected control levels (23.7 ± 7.2 ng/mg total protein) in all genotypes (Figure 6).
However, C3 levels returned to control levels (22.0 ± 2.6 ng/mg total protein) at 3 days after the last LPS-injection in all genotypes, showing that the acute inflammatory response last only for 1-3 days.
Thus, while there is a clear immune response to peripheral LPS injections in the brain, including increased levels of C3 protein, this response did not differ amongst all genotypes.

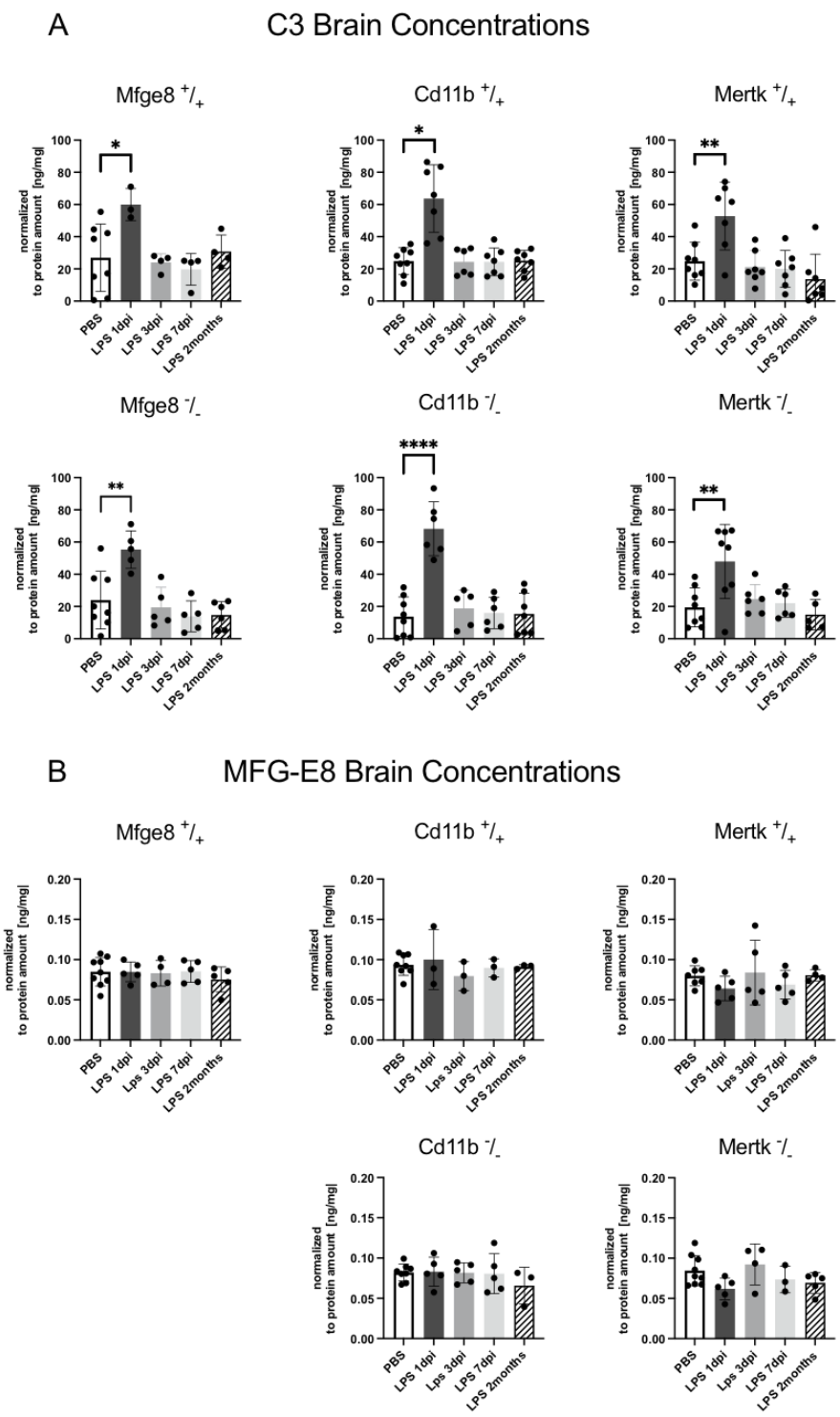

Figure 6: Brain concentration of phagocytic proteins

A) Complement protein 3 (C3) brain concentrations were measured in different phagocytic deficient mouse strains and wildtype controls using ELISA method. C3 levels increased strongly 1 day after two i.p. LPS-injections compared to PBS-injected control levels in all genotypes and returned to baseline levels 3 days post-injection.
Data shown are means ± SD and normalized to brain protein amount, PBS-treated animals of all timepoints were pooled.
* p<0,05, ** p< 0,01, ***p< 0,001, *** p< 0,0001, **** p<0,00001. Ordinary One-Way Anova and Tukey's multiple comparison test was performed for all groups except for *Cd11b* $^{+}/_{+}$. For *Cd11b* $^{+}/_{+}$ Kruskal-Wallis-Test and Dunn's multiple comparison test was executed. For PBS/ LPS 1dpi/ LPS 3dpi/ LPS 7dpi/ LPS 2months n=8/6/7/7/7 for *Mfge8* $^{+}/_{+}$, n=8/5/5/5/6 for *Mfge8* $^{-}/_{-}$; n= 8/7/6/7/7 for *Cd11b* $^{+}/_{+}$, n= 8/6/5/6/7 for *Cd11b* $^{-}/_{-}$*, n= 8*/7/7/7/7 for *Mertk* $^{+}/_{+}$*, n=8/8/6/6/5 for Mertk* $^{-}/_{-}$ (1 Outlier in *Mfge8* $^{+}/_{+}$ LPS 7dpi and *Mertk* $^{+}/_{+}$ LPS 2 months not shown.)

B) Milk fat globule EGF-like factor 8 (MFG-E8) concentrations were measured using ELISA. MFG-E8 levels were indistinguishable after LPS-administration in phagocytic deficient or wildtype mice in comparison to PBS-injected controls of all timepoints.
Data shown are means ± SD and normalized to brain protein amount, PBS-treated animals of all timepoints were pooled.
For PBS/ LPS 1dpi/ 3dpi/ 7dpi/ 2 months n=9/5/4/5/5 for *Mfge8* $^{+}/_{+}$; n=8/3/3/3/3 for *Cd11b* $^{+}/_{+}$; n=8/5/5/5/3 for *Cd11b* $^{-}/_{-}$; n=8/5/5/5/4 for *MerTK* $^{+}/_{+}$; n=9/5/4/3/5 *Mertk* $^{-}/_{-}$ (1 Outlier in *Mertk* $^{+}/_{+}$ PBS and LPS 2 months not shown)

4.1.2 Milk fat globule EGF-like factor 8 levels are not altered in the brain after simulated sepsis

To test the influence of LPS-induced immune activation on MFG-E8 expression, MFG-E8 protein concentration was measured in the brain at different timepoints after i.p. LPS-injections. In contrast to C3 levels, no significant increase of MFG-E8 protein levels were detected after one day (0.08 ± 0.02 ng/mg total protein), three days (0.08 ± 0.005 ng/mg total protein), seven days (0.08 ± SEM 0.009 ng/mg total protein) nor 2 months (0.08 ± 0.01 ng/mg total protein) in phagocytic deficient or wildtype mice in comparison to PBS-injected controls (0.09 ± 0.005 ng/mg total protein) of all timepoints (Figure 6).
Thus, while MFG-E8 protein levels remained constant following peripheral LPS-injections, a shift from intra- to extracellular location could still occur (as MFG-E8 is normally secreted) to increase extracellular MFG-E8 levels while the total concentration remains constant. To further understand, whether this is indeed the case, further tests should be conducted.

4.1.3 Microglia volume increases acutely after sepsis

The microglia cell volume is another measure of microglial activation and was analyzed here using 3-dimensional reconstructions with Imaris (Bitplane). As expected, in all genotypes, one to three days after LPS-injections, microglia volume was strongly increased in cortex (*Mfge8* $^{+}/_{+}$: LPS 1d: 1.4 ± 0.5 and LPS 3d: 1.5 ± 0.6; *Mfge8* $^{-}/_{-}$: LPS 1d: 2.1 ± 0.5 and LPS 3d: 1.9 ± 0.4; *Cd11b* $^{+}/_{+}$: LPS 1d: 2 ± 0.8 and LPS 3d: 1.9 ± 0.7; *Cd11b* $^{-}/_{-}$: LPS 1d: 2 ± 0.3 and LPS 3d: 1.7 ± 0.4 μm^3) compared to PBS-injected control group (*Mfge8* $^{+}/_{+}$: 1 ± 0.15; *Mfge8* $^{-}/_{-}$: 1 ± 0.2; *Cd11b* $^{+}/_{+}$: 1 ± 0.3; *Cd11b* $^{-}/_{-}$: 1.0 ± 0.2 μm^3) and in CA1 (*Mfge8* $^{+}/_{+}$: LPS 1d: 1.4 ± 0.1 and LPS 3d: 1.5 ± 0.6; *Mfge8* $^{-}/_{-}$: LPS 1d: 2 ± 0.4 and LPS 3d: 2 ± 0.5; *Cd11b* $^{+}/_{+}$: LPS 1d: 2.1 ± 0.5 and LPS 3d: 1.7 ± 0.4; *Cd11b* $^{-}/_{-}$: LPS 1d: 2 ± 0.3 and LPS 3d: 1.5 ± 0.2 μm^3) compared to PBS-injected control group (*Mfge8* $^{+}/_{+}$: 1 ± 0.08; *Mfge8* $^{-}/_{-}$: 1 ± 0.07; *Cd11b* $^{+}/_{+}$: 1 ± 0.1; *Cd11b* $^{-}/_{-}$: 1.0 ± 0.2 μm^3).

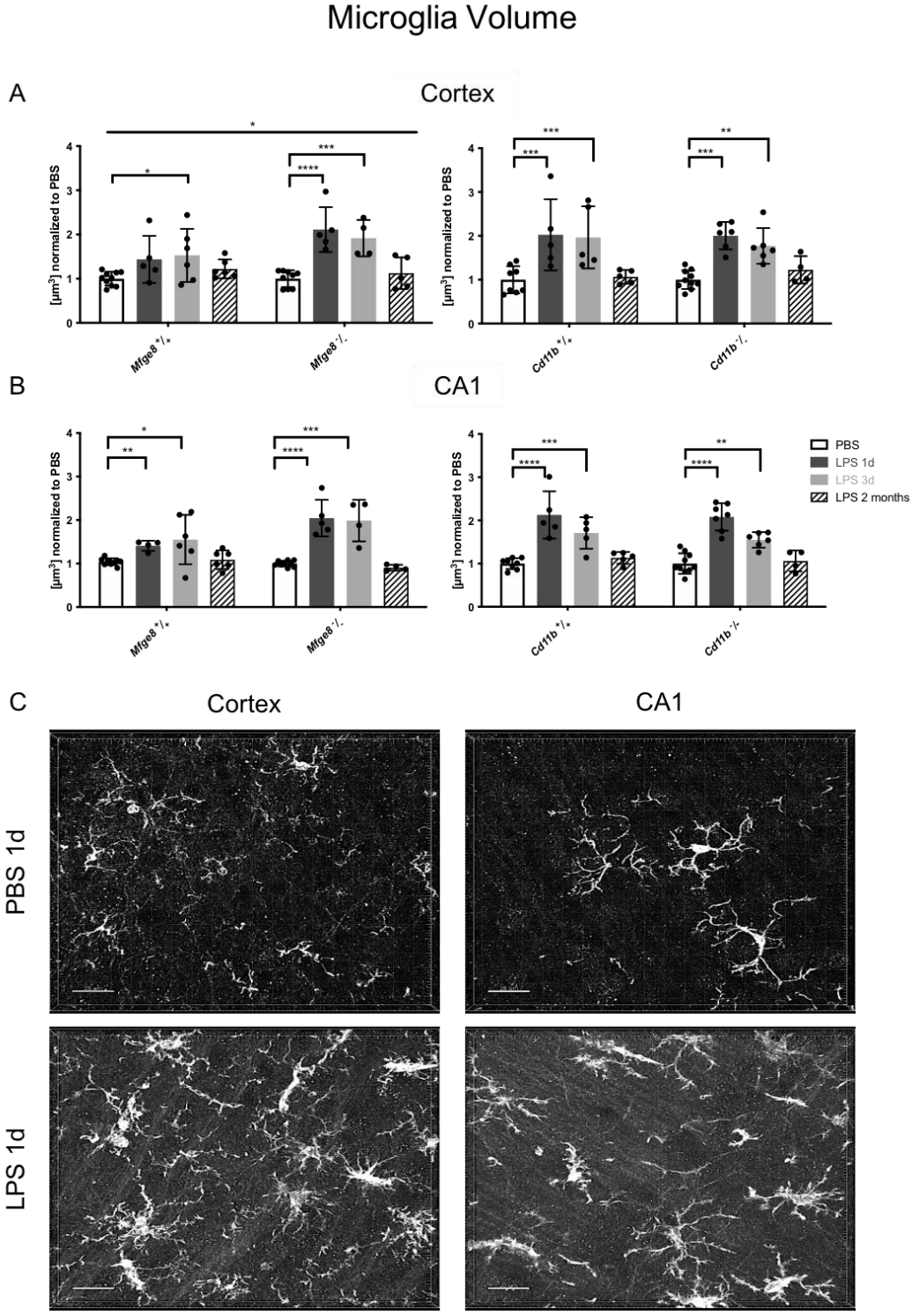

Figure 7: Microglial cell volume changes following peripheral LPS-stimulation

A) In cortex, acutely after LPS-injections, microglia volume is increased in *Mfge8* wildtype and knockout as well as in *CD11b* wildtype and knockout mice.
Data shown are means ± SD and normalized to PBS, two way-ANOVA with post-hoc test (Dunnett's multiple comparison test) was performed. PBS-treated animals of all timepoints were pooled. * p< 0,05, ** p< 0,01, *** p< 0,001; **** p< 0,0001
For PBS/ LPS 1dpi/ LPS 3dpi/ LPS 2months n=9/5/6/6 for *Mfge8* $^{+}/_{+}$, n=9/5/4/5 for *Mfge8* $^{-}/_{-}$; n= 8/5/5/5 for *Cd11b* $^{+}/_{+}$, n= 10/7/6/4 for *Cd11b* $^{-}/_{-}$ (1 Outlier in *Cd11b* $^{+}/_{+}$ LPS 1dpi not shown)

B) In CA1, microglia volume is also acutely increased in *Mfge8* wildtype and knockout and in *Cd11b* wildtype and knockout.
Data shown are means ± SD and normalized to PBS, two way-ANOVA with post-hoc test (Dunnett's multiple comparison test) was performed. PBS-treated animals of all timepoints were pooled. * p< 0,05, ** p< 0,01, *** p< 0,001; **** p< 0,0001
For PBS/ LPS 1dpi/ LPS 3dpi/ LPS 2months n=10/6/5/5 for *Mfge8* $^{+}/_{+}$, n=9/5/4/6 for *Mfge8* $^{-}/_{-}$, n= 8/5/5/5 for *Cd11b* $^{+}/_{+}$, n= 10/7/6/4 for *Cd11b* $^{-}/_{-}$ (1 Outlier in *Mfge8* $^{+}/_{+}$ PBS, LPS 1dpi and *Mfge8* $^{-}/_{-}$ LPS 2 months not shown)

C) Representative IBA-1 positive staining of *Cd11b* wildtype. (Scalebar 20 µm)

As reported previously, after activation by different immune stimuli, microglia volume is increased [38]. Therefore, it seems that LPS-injections in the peritoneum is also sufficient to mimic an inflammatory process for microglia (Figure 7).

4.1.4 Non-significant increase in brain and ventricle volume

To further analyze the reaction of the brain to peripheral immune stimulation by LPS-injections, volume of different brain structures was measured using Fiji.
The analysis of the cresyl violet stained slices did not show any significant increase or decrease in the volume of different brain regions. The slight increase in hemisphere volume 1 day (LPS 0.6 ± 0.1 vs. PBS 0.5 ± 0.05 mm^3) and cortex volume (LPS 0.2 ± 0.08 vs. PBS 0.2 ± 0.02 mm^3) post injection might be due to acute inflammatory swelling. Of note, edema and increasing intracranial brain pressure (ICP) is often observed in septic patients. [29, 92, 93] However, a non-significant increase in dentate gyrus (DG), hippocampal regions, one day (LPS 0.002 ± 0.0007 vs. PBS 0.001 ± 0.0001 mm^3) after LPS exposure could be observed (Figure 8).
Interestingly, the total ventricle volume was strongly, but non-significantly increased one day after LPS-induced sepsis (LPS 0.006 mm^3 ± 0.003 vs. PBS 0.003 mm^3 ± 0.001). As it has been found, that secretory epithelia respond to cytokines and pro-inflammatory signals [94], this increase in ventricle volume could be due to an increase in cerebrospinal fluid (CSF).

To sum up, peripheral LPS-injections lead to an acute inflammatory response in the brain, as C3 is highly expressed and also microglia volume is significantly increased. Furthermore, a slight increase in ventricle volume could be observed as well as an increase in total brain volume. This might be due to acute swelling of the brain and increased CSF production as a reaction to the inflammation [92].

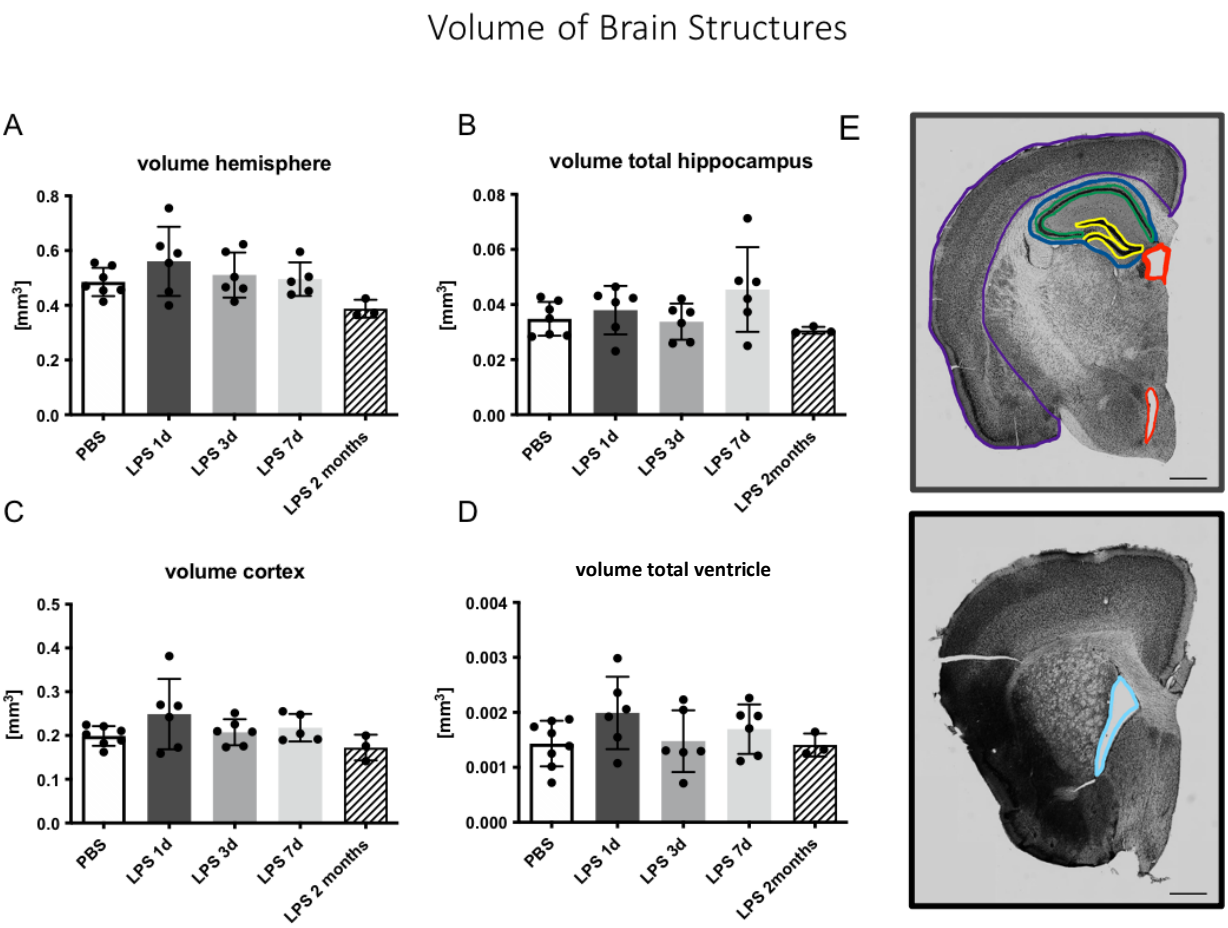

Figure 8: Volume of brain structures

A) Hemisphere volume of C57BL/6 mice were quantified using Fiji. A non-significant increase in hemisphere volume 1 day after LPS-injections was found. This might be due to acute inflammatory swelling.
B) A non-significant increase was seen for dentate gyrus (DG) volume.
C) Cortex volume is non-significantly increased 1 day post injection.
D) Also, a non-significant increase in total ventricle volume (sum of first and third ventricle volume) one day after LPS-induced sepsis was observed.
E) In violet volume of cortex, in dark blue total hippocampus volume, in green volume of CA1, in yellow volume of DG, in red volume of third ventricles and in light blue volume of first ventricle is highlighted. Data for volume of CA1 is not shown because no increase was found after LPS-injections. (Scale bar: 100 µm).
Cresyl violet staining was done by Maren Lösch, imaging, analysis and statistics were done by the author.
Data shown are means ± SD, PBS-treated animals of all timepoints were pooled. $n_{LPS}=6$; $n_{PBS}=2$

4.2 Long-term effects of i.p LPS-injections to cytokine brain levels

Because the previous analyses did not reveal any sign of long-term changes in opsonin levels or microglia morphology after sepsis, different cytokines concentrations were measured in wildtype and knockout mice two months after two consecutive LPS-injections, to see whether long-term alterations in the

brain's inflammatory status could be seen using a highly sensitive multiplex ELISA.

Interestingly, in *Cd11b* knockout mice, anti-inflammatory cytokine interleukin (IL)-4 levels were found to be increased in comparison of LPS-treated (0.08 ± 0.01 pg/mg) to PBS-treated animals (0.04 ± 0.02 pg/mg), while *Cd11b*, *Mfge8* and *Mertk* wildtype as well as *Mfge8* and *Mertk* knockout mice showed no significant difference in IL-4.

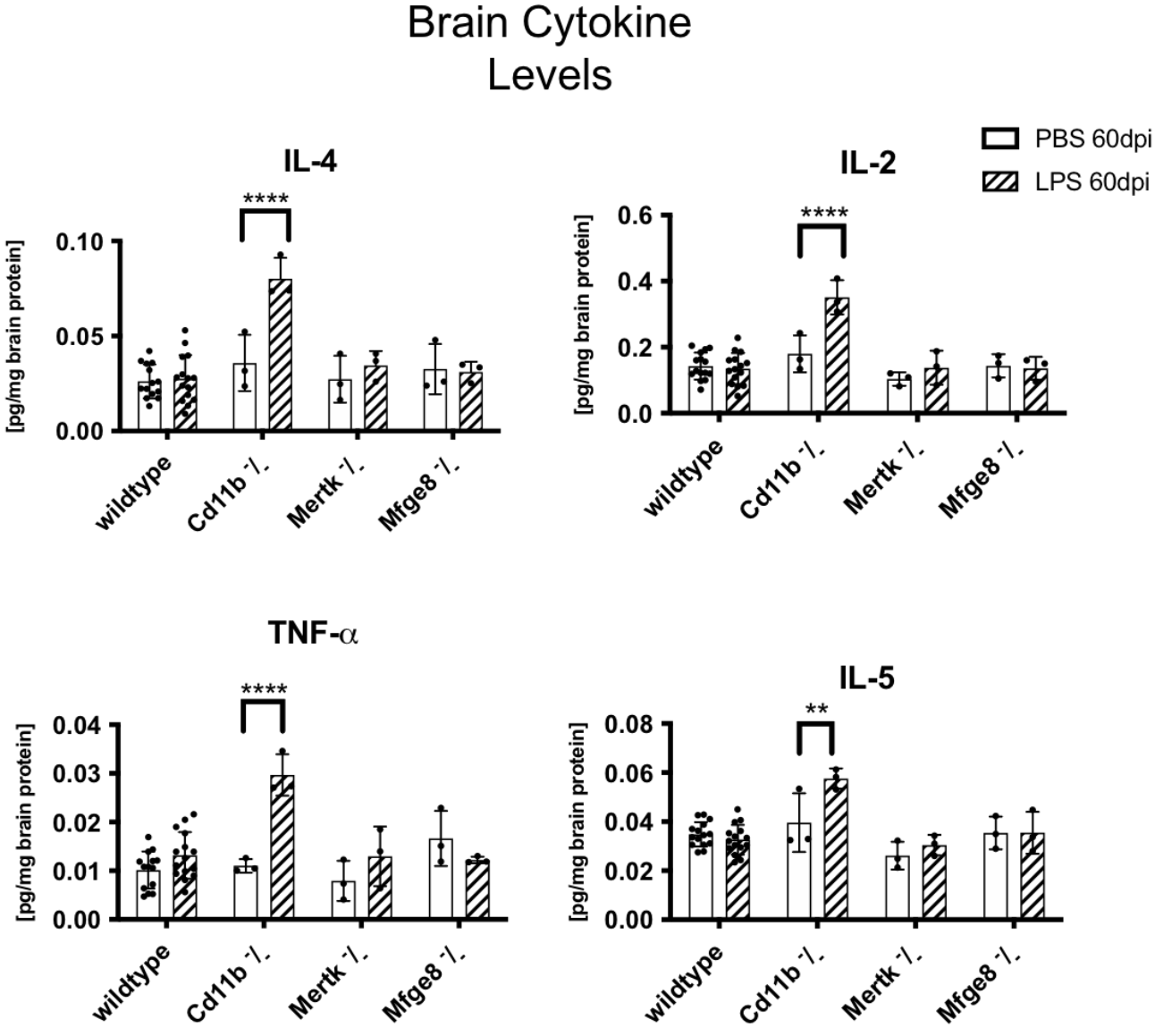

Figure 9: Brain cytokine levels 2 months after LPS injections

Only *Cd11b* knockout show an increase in different cytokine levels two months after LPS-injections.
Data shown are means ± SD and normalized to brain protein amount, Mertk, *Cd11b* and *Mfge8* $^{+/+}$ were grouped as wildtype, two way-ANOVA with post-hoc test (Šídák's multiple comparisons test) was performed. ELISA protocol was carried out by Lisa Häsler and Rawaa Al-Shaana, analysis and statistics were done by the author.
** p< 0,01, **** p< 0,0001, $n_{wildtype}$= 15, $n_{knockout}$= 3.

In pro-inflammatory cytokine levels, tumor necrosis factor (TNF)-α, interferon (IFN)-γ, IL-2 and IL-5 were also significantly increased in LPS-treated *Cd11b* knockout mice in comparison to control group (LPS vs. PBS for TNF-α: 0.03 ± 0.002 vs. 0.01 ± 0.001 pg/mg; INF-γ: 0.04 ± 0.002 vs 0.01 ± 0.006; IL-2: 0.4 ± 0.05 vs. 0.18 ± 0.06; IL-5: 0.06 ± 0.004 vs. 0.04 ± 0.01). In *Cd11b* wildtype, TNF-α concentration was also increased two months after LPS injections (LPS 0.02 ± 0.007 vs. PBS 0.01 ± 0.003 pg/mg) (Figure 9).

Interestingly, like in anti-inflammatory cytokine levels, pro-inflammatory cytokines are only increased in *Cd11b* knockout mice. All other genotypes do not differ significantly between wildtype and knockout mice. Also, no difference at all was observed in pro-inflammatory keratinocyte chemoattractant (KC)/ human growth-regulated oncogene (GRO) and IL-1β.

In summary, only *Cd11b* knockout mice were found to have increased pro- and anti-inflammatory cytokine levels two months after double i.p. LPS-injections. Cd11b is expressed in macrophages, dendritic cells and neutrophils and is important for migration and function of leucocytes [70]. It has been found, that Cd11b is important in controlling LPS-induced Toll-like receptor (TLR) signaling in innate immune response and therefore is preventing an overreaction of the immune system [95]. Therefore, the finding that only in *Cd11b* knockout mice a long-term difference in pro-inflammatory cytokines could be detected, might be explained through the missing alleviative effect of Cd11b on TLR-mediated immune activation after LPS-injections.

4.3 Functional synapse number is decreased acutely and increased long-term after sepsis

To determine whether synaptic remodeling was affected in our model of sepsis, functional synapse number, defined as colocalization of pre- and postsynaptic proteins, was analyzed using FIJI.

In *Mfge8* wildtype animals functional synapse number is strongly decreased acutely (Cortex: LPS 1d: 0.4 ± 0.2 and LPS 3d: 0.7 ± 0.2 vs. PBS 1 ± 0.2; CA1: LPS 1d: 0.3 ± 0.09 and LPS 3d: 0.4 ± 0.2 vs. PBS 1 ± 0.1) after sepsis. The synapse number is normalizing over two months post injections in cortex. However, in the CA1 region, synapse number remains significantly decreased two months (LPS 0.6 ± 0.1 vs. PBS 1 ± 0.1) after sepsis.
Interestingly, loss of functional synapse number could be prevented in *Mfge8* knockout mice in cortex (LPS 1d: 0.8 ± 0.3 and LPS 3d: 0.9 ± 0.3 vs. PBS 1 ± 0.2) and CA1 (LPS 1d: 0.8 ± 0.2 and LPS 3d: 0.9 ± 0.2 vs. PBS 1 ± 0.2), indicating for the first time that MFG-E8 plays a role in marking synapses for removal during brain inflammation (Figure 10).

Surprisingly, for *Cd11b* animals, no strong decrease acutely after sepsis could be observed either in wildtype (cortex: LPS 1d: 0.8 ± 0.2 and LPS 3d: 0.7 ± 0.2 vs. PBS 1 ± 0.5; CA1: LPS 1d: 1 ± 0.3 and LPS 3d: 1 ± 0.2 vs. PBS 1 ± 0.3) nor knockout mice (cortex: LPS 1d: 1 ± 0.4 and LPS 3d: 0.9 ± 0.3 vs. PBS 1 ± 0.2; CA1: LPS 1d: 1 ± 0.5 and LPS 3d: 1 ± 0.4 vs. PBS 1 ± 0.2). Strikingly, in wildtype mice two months after LPS-injections synapse number was significantly increased in cortex (LPS 1.6 ± 0.3 vs. PBS 1 ± 0.5) and non-significantly increased in CA1 region (LPS 1.3 ± 0.7 vs. PBS 1 ± 0.3).

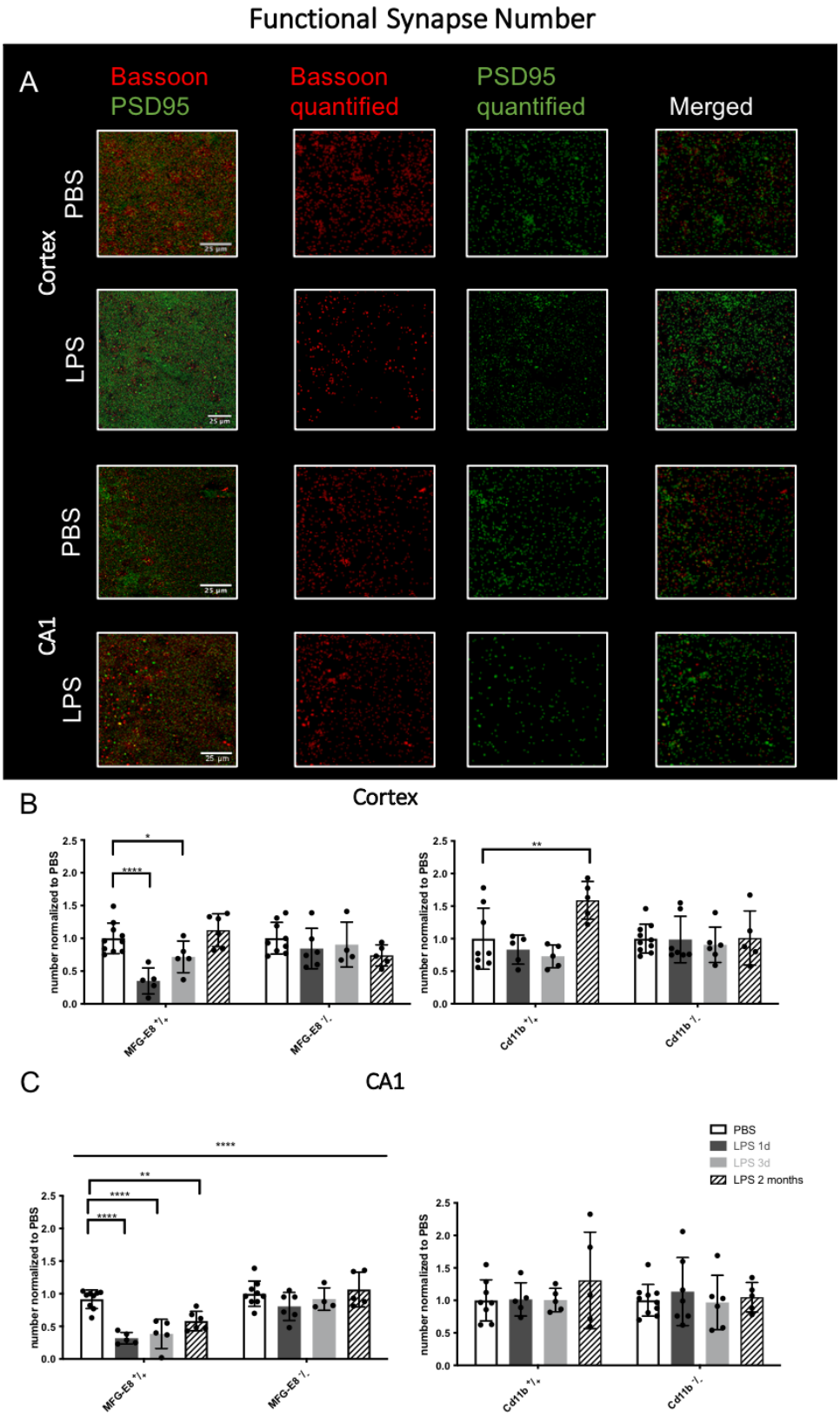

Figure 10: Functional synapse number

A) Representative images of *Mfge8* wildtype animals 1 day after two consecutive LPS-injections. The tissue was stained for Bassoon (red) and PSD95 (green) and functional synapse area was analysed using Puncta Analyzer by Bary Wark. The original image and the quantified synapses are depicted. Scale bar: 25µm

B) In cortex, *Mfge8* wildtype animals synapse number is strongly decreased 1 day after LPS-injections, whereas *Cd11b* wildtype show no significant reduction. Synapse number is increased in *Cd11b* wildtype animals two months after sepsis. *Mfge8* and *Cd11b* knockout do not show differences in synapse number acutely or long-term after sepsis.
Data shown are means ± SD and normalized to PBS, two way-ANOVA with post-hoc test (Dunnett's multiple comparison test) was performed. PBS-treated animals of all timepoints were pooled. * p< 0,05; ** p< 0,01, **** p< 0,0001 For PBS/ LPS 1dpi/ LPS 3dpi/ LPS 2months n=10/5/5/6 for *Mfge8* $^{+}/_{+}$, n=9/6/4/5 for *Mfge8* $^{-}/_{-}$; n= 8/5/5/5 for *Cd11b* $^{+}/_{+}$, n= 10/7/6/5 for *Cd11b* $^{-}/_{-}$

C) In CA1, a significant decrease in synapse number in *Mfge8* wildtype mice could be detected.
Data shown are means ± SD and normalized to PBS, two way-ANOVA with post-hoc test (Dunnett's multiple comparison test) was performed. PBS-treated animals of all timepoints were pooled. * p< 0,05; ** p< 0,01, **** p< 0,0001. For PBS/ LPS 1dpi/ LPS 3dpi/ LPS 2months n=10/5/5/6 for *Mfge8* $^{+}/_{+}$, n=9/6/4/5 for *Mfge8* $^{-}/_{-}$; n= 8/5/5/5 for *Cd11b* $^{+}/_{+}$, n= 10/7/6/5 for *Cd11b* $^{-}/_{-}$ (1 Outlier in *Mfge8* $^{-}/_{-}$ PBS not shown).

4.4 Phagocytosis of functional synapses is increased acutely after sepsis

To investigate whether the loss of functional synapses could be explained by phagocytosis, colocalization of pre- and postsynaptic puncta inside microglia were analyzed using Imaris (Bitplane).

As the phagocytosed synaptic puncta are clustered inside the microglia, the volume of phagocytosed synapses was also analyzed (Figure 11).

Table 4: Phagocytosed synapse volume

	Mfge8 $^{+}/_{+}$		*Mfge8* $^{-}/_{-}$		*Cd11b* $^{+}/_{+}$		*Cd11b* $^{-}/_{-}$	
	PBS 1-3d	LPS 1d	PBS 1-3d	LPS 1d	PBS 1-3d	LPS 1d	PBS 1-3d	LPS 1d
Cortex	159 ± 14	170 ± 57	53 ± 9	80 ± 12	25 ± 3	128 ± 21	33 ± 3	82 ± 17
CA1	121 ± 25	140 ± 62	79 ± 31	96 ± 15	27 ± 6	108 ± 22	37.2 ± 6	108 ± 23

Average of phagocytosed synapse volume per timepoint for *Mfge8* and *Cd11b* wildtype and knockout is shown in [μm^3].

No increase in phagocytosis of synaptic proteins could be observed acutely after LPS-induced sepsis in *Mfge8* wildtype mice, however in *Cd11b* wildtype a strong increase was seen acutely after sepsis. The lack of increase in *Mfge8* wildtype animals may be an artefact, due to insufficient cryoprotection (as mentioned in 3.6.1). In *Mfge8* wildtype only three PBS-treated animals from one to three days post injection could be used for analysis. As shown in Table 4, PBS-treated *Mfge8* wildtype animals show already a very high value of phagocytosed synapse volume compared to *Cd11b* wildtype animals. Therefore, the lack of increased phagocytic activity in *Mfge8* wildtype mice might be an artefact due to insufficient tissue quality of PBS-treated *Mfge8* animals. To further prove this assumption more PBS-treated wildtypes animals should be analyzed. Unfortunately, for further analysis new animals would have to be treated, which is not possible at

the moment. However, other effects, e.g. batch effects, cannot be excluded at the moment.

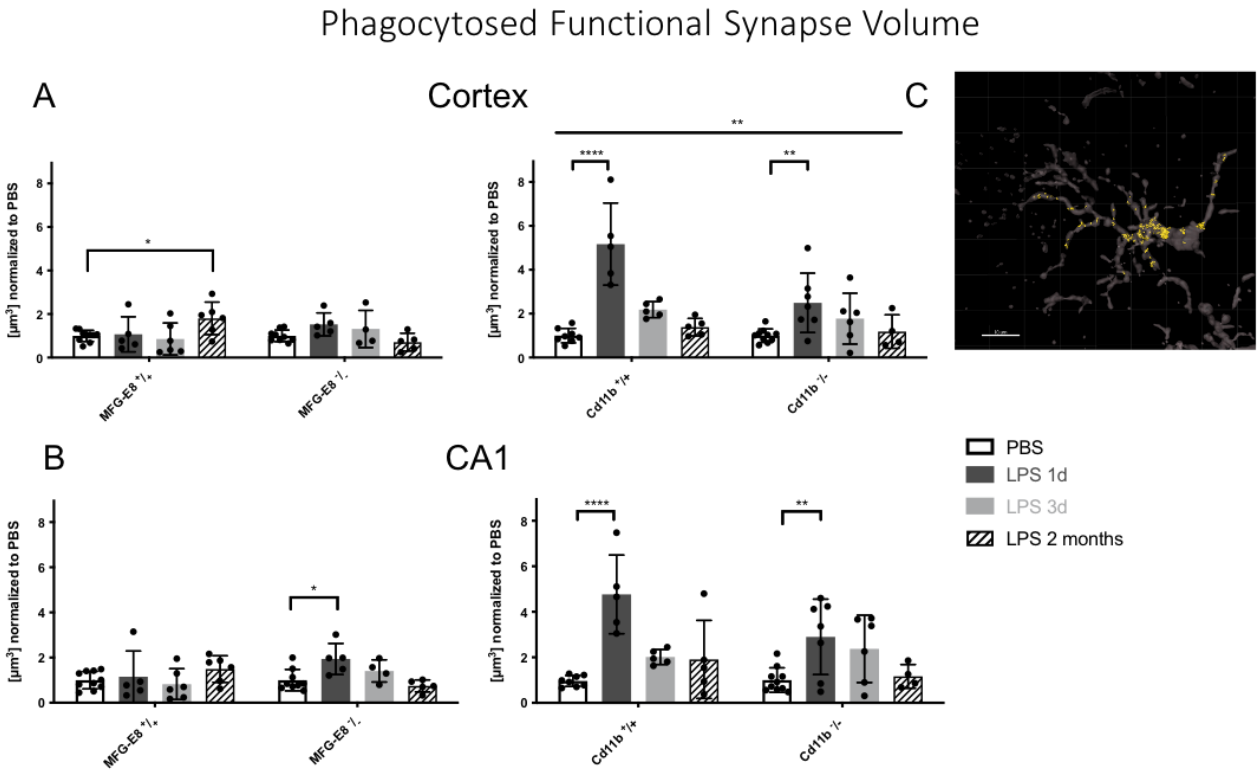

Figure 11: Phagocytosed synapse volume

A) In the cortex, phagocytosed synapse volume is increased 2months after LPS-injections in *Mfge8* wildtype animals. Whereas in *Cd11b* wildtype and knockout mice, phagocytosed functional synapse volume is significantly increased 1 day after two LPS-injections.
Data shown are means ± SD and normalized to PBS, two way-ANOVA with post-hoc test (Dunnett's multiple comparisons test) was performed. PBS-treated animals of all timepoints were pooled. * p< 0,05, ** p< 0,01, **** p< 0,0001
For PBS/ LPS 1dpi/ LPS 3dpi/ LPS 2months n=10/5/6/6 for *Mfge8* $^{+}/_{+}$; n=9/5/4/5 for *Mfge8* $^{-}/_{-}$; n=8/5/5/5 for *Cd11b*$^{+}/_{+}$; n=10/7/6/4 for *Cd11b* $^{-}/_{-}$

B) In CA1, phagocytosis is only increased in *Mfge8* knockout mice 1 day after sepsis. In *Cd11b* wildtype and knockout mice show an increased phagocytosis one day after two LPS-injections.
Data shown are means ± SD and normalized to PBS, two way-ANOVA with post-hoc test (Dunnett's multiple comparisons test) was performed. PBS-treated animals of all timepoints were pooled. * p< 0,05, ** p< 0,01, **** p< 0,0001
For PBS/ LPS 1dpi/ LPS 3dpi/ LPS 2months n=10/5/6/6 for *Mfge8* $^{+}/_{+}$; n=9/5/4/5 for *Mfge8* $^{-}/_{-}$; n=8/5/5/5 for *Cd11b*$^{+}/_{+}$; n=10/7/6/4 for *Cd11b* $^{-}/_{-}$

For *Mfge8* knockout mice a slight increase in engulfed synaptic proteins could be observed in cortex (Fig. 11: LPS 1d: 1.5 ± 0.5 vs. PBS 1 ± 0.2) and CA1 (LPS 1d: 2 ± 0.7 vs. PBS 1 ± 0.5), which is also represented in a non-significant decrease in functional synapse number (Fig. 10: LPS 1d: cortex: 0.8 ± 0.3 vs. PBS 1 ± 0.2; CA1: 0.8 ± 0.2 vs. PBS 1 ± 0.2). However, the absolute volume of acutely phagocytosed synapses was reduced compared to *Mfge8* wildtype animals (Table 4). Therefore, loss of MFG-E8 seems to reduce the phagocytosis of

functional synaptic puncta, even under homeostatic conditions. However, further analysis has to be carried out to further validate these results.

As for *Cd11b* wildtype animals, in *Cd11b* knockout mice a significant increase in phagocytosis was detected acutely after LPS-injections (LPS 1d Cortex: 2.5 ± 1.4 vs. PBS 1 ± 0.3; LPS 1d CA1: 3 ± 1.7 vs. PBS 1 ± 0.5 μm^3). Interestingly, similar to *Mfge8* knockout mice, *Cd11b* knockout animals showed a reduced uptake of synapses acutely after sepsis (Table 4).
In *Mfge8* wildtype mice, only in the cortex a sustained increase in phagocytosis two months after LPS-induced sepsis could be seen (LPS 1.8 ± 0.7 vs. PBS 1.0 ± 0.3). However, in CA1 as well as in *Mfge8* knockout and *Cd11b* wildtype and knockout mice, phagocytosis of synapses was unchanged following LPS injections (LPS vs. PBS for *Mfge8* $^{+}/_{+}$ CA1: 1.5 ± 0.6 vs. 1 ± 0.4; *Mfge8* $^{-}/_{-}$ Cortex: 0.7 ± 0.4 vs. 1 ± 0.3; *Mfge8* $^{-}/_{-}$ CA1: 0.7 ± 0.3 vs. 1 ± 0.5; Cd11b $^{+}/_{+}$ Cortex: 1.4 ± 0.4 vs. 1 ± 0.3; Cd11b $^{+}/_{+}$ CA1: 1.9 ± 1.7 vs. 1 ± 0.2; Cd11b $^{-}/_{-}$ Cortex: 1.2 ± 0.8 vs. 1 ± 0.3; Cd11b $^{-}/_{-}$ CA1: 1.2 ± 0.5 vs. 1 ± 0.5) (Figure 11).

To sum up, under assumption that the phagocytosed volume of PBS-treated *Mfge8* wildtype animals is an artefact due to low tissue quality, *Mfge8* and *Cd11b* wildtype animals show an increased phagocytosis acutely after LPS-induced sepsis, which is partly prevented in the corresponding knockout animals. Further analysis could test, whether complete knockout of both proteins could prevent phagocytosis of synapses completely. Further investigation why only in the cortex of *Mfge8* wildtype mice a sustained increase in phagocytosis following sepsis was found and not in CA1 or *Cd11b* wildtype animals may provide further insight in the pathophysiological role of these opsonins.

5 Discussion

Many survivors of severe sepsis show long-lasting cognitive impairment, which leads to reduced quality of life and dependency on long-term care [24, 25]. Different pathologies leading to this impairment like brain atrophy, white matter loss [26-28] as well as activation and proliferation of microglia cells [30], have been discovered until now. However, the interrelations between microglia activation, brain atrophy and long-term cognitive deficits have not been researched so far. To investigate a possible correlation, we conducted this study to observe the role of microglia in synapse degeneration following LPS-induced sepsis.

This study shows that peripheral LPS injections stimulate the innate immune system in the brain, as indicated by increasing C3 concentrations and microglia volume. Additionally, in *Mfge8* and *Cd11b* wildtype mice, synapse loss and correspondingly an increase in synaptic pruning was detected days after LPS injections, which was partly prevented in knockout mice. However, contrary to our expectations, no cellular correlate of long-term cognitive impairments, e.g. persistent reduction in synapse number or increased phagocytosis, was evident in the immunohistochemical analysis of the brains.

5.1 Behavioral analysis showed that inhibition of phagocytosis protects against long-term cognitive deficits

In addition to the biochemical and immunohistochemical analysis described above, behavioral analysis conducted by a collaborating group in Berlin (AG Emmrich) was performed to assess the short- and longterm impact of LPS-injections on the animal's physiology and cognition [89]. The mice were tested in different behavioral setups after one month of resting (Figure 5). To evaluate physiological changes after LPS-injections, for up to 28 days after the injections body temperature and weight were registered. Furthermore, sickness behavior was analyzed by investigating the ability to build a nest by a definitive 5 points

nest-rating scale [96]. Also, the activity of the animals was observed by using day-long video recording and tracking of the caged animals. These analyses revealed a strong increase in body temperature, as well as a loss of bodyweight, daily activity and decrease of nest building score after LPS-injections. These reactions have been described previously and are known to be a common reaction of the host to inflammation [97-100]. The strong reactions observed in the mice after the LPS-injections prove that the administered amount of LPS is sufficient to simulate a severe sepsis in all mice. Furthermore, cytokine measurements in the serum of mice also showed the expected acute increase of inflammation markers in all genotypes, with no effects apparent between the different wildtype and knockout lines (unpublished data of the host laboratory). Altogether, this shows that the administrated amount of LPS is sufficient to induce a systemic sepsis-like state in all mice independent of genotype. Additionally, this proves that the knockout of phagocytic proteins has no effect in the early systemic inflammation phase after LPS-injections, but rather leads to a specific reduction of microglia-mediated phagocytosis.

By using IntelliCage [101-103] (TSE Systems GmbH, Bad Homburg, Germany), a monitored system housing 8-16 transponder-targeted mice, spontaneous explorative behavior and circadian rhythm was monitored over a period of 7 days without human interference to further test for spatial and affective memory deficits after LPS-injections. Independent of genotype, LPS-treated wildtype animals showed a decreased ability in spatial learning for at least the measured 4 days. However, for spatial memory ability, clear tendencies, that LPS-treated wildtype animals were more impaired compared to knockout animals were found (e.g. *Mfge8* knockout animals performed better in avoidance conditioning, *Mertk* knockout mice in place learning and reversal and *Cd11b* knockout mice showed an increase in explorative behavior). Moreover, animals subjected to experimental sepsis showed a significant reduction in avoidance behavior, which also suggest that these mice may suffer from impairments in their affective memory after LPS-injections. However, it remains unclear why different knockout

mice show improved results in different tests. Further investigations will be necessary to explain this effect.

In summary, although no clear cellular correlate of long-term cognitive impairments was found in the tissue analysis conducted here, the behavioral testing clearly demonstrated that mice after LPS injections showed acutely severe sickness behavior and long-term impairments in spatial and affective memory compared to PBS-injected animals. As well as the synapse loss by phagocytosis, the decline in cognitive functions was partly rescued by knockout of phagocytic proteins.

5.2 Induction of microglial overactivation after i.p. LPS-injections

Microglia have been found to be not only necessary for synaptic pruning during development and network formation in the young and adult brain but also in brain diseases [74, 104]. A common feature of neurodegenerative diseases despite the different underlying pathologies is an early synaptic loss which leads to network and synaptic dysfunction [39, 73, 104]. In neurodegenerative diseases a genetic vulnerability, e.g. mutation in triggering receptor expressed on myeloid cells 2 (TREM2), is assumed to induce microglial dysfunction and impaired phagocytosis. The accumulating tissue debris then induces microglial activation and inflammatory responses, which complete the vicious cycle through neuronal damage and increased production of debris [105]. Taking this in consideration, our findings might suggest that the inflammation following sepsis can also induce a vicious cycle of microglial overactivation without a preliminary genetic vulnerability, suggesting that sepsis-induced synaptic pruning reduced synaptic connections and thus cognitive dysfunction.

This study demonstrates that within 7 days after two consecutive LPS-injections, synapse number, synaptic phagocytosis as well as microglial activation is normalized. This apparent return to baseline correlated with the

termination of inflammation (as evidenced for example by cytokine levels). Therefore, microglia activation, phagocytosis and synapse loss as well and synapse number appears to be able to fully recover. The brain is known to be able to react to different internal or external stimuli by undergoing functional and morphological changes via mechanisms of plasticity in order to encode memories[106]. This neuronal plasticity has also been identified as an important feature of the brain to cope with neuronal and synapse loss after diseases, e.g. stroke. Despite worse long-term prognosis for survivors of stroke [107, 108], patients show a steady improvement in memory, motor and cortical functions months after stroke [109]. It has been discussed that several mechanisms play an important role in synapse recovery and network formation [106]. These mechanisms show differences in their time course. Synaptic regeneration is thought to take hours or days[110] and might be the mechanism behind this early recovery process.

Although on a cellular level, parameters for microglial activation, synapse number and phagocytosis of synapses normalized within about one week after sepsis, treated animals showed long-term cognitive impairment two months after peripheral LPS injections. This change might be due to a more long-term plasticity mechanism called synaptic reorganization and cortical remapping, which is known to take months after neuronal loss [110]. In this way, and although the synapse number is normalized two months after sepsis, it might be possible that correct neuronal circuits and synaptic functions are not established again and functional deficits remain. However, further electrophysiological and functional analysis is needed to evaluate changes in neuronal circuits.

While the LPS animal model for sepsis shows better reproducibility and standardization, two separate LPS injections are not sufficient to mimic the complex and long-lasting immunological stimulus of bacteremia during sepsis. Assuming that the intensity of the immunological stimulus correlates with the extent of synaptic loss and phagocytosis, a continuous inflammatory state that last several days, as achieved by CLP or other sepsis models, might damage the neuronal circuits to a greater extent than two consecutive LPS-injections. Therefore, it may be possible that the mechanism of synaptic regeneration is in

this case not sufficient to recover the synapse number completely. Therefore, immunohistological experiments using alternative sepsis models may be able to detect the changes underlying the long-lasting synaptic deficiency which was detected in the behavioral tests.

Additionally, one major risk factor for long-term cognitive impairments following critical illness is an advanced age [111]. It is known that during aging, microglia are in a more activated state and show an enhanced inflammatory response to pathologies [112-114]. As the mice were injected at two to three months of age and tested for up to two months, the long-term effects of sepsis were tested with four to five months old mice, which is considered equal to being a young adult. To exclude that long-term deficits will become immunohistologically apparent in older individuals, equal experiments should be carried out with older mice.

Microglia are known to be crucial for synaptic pruning in the developing brain. But just recently, Wang et al showed in a mouse study that microglia do not only mediate synaptic refinement during development but also induce activity-mediated memory loss by synaptic pruning in healthy brains, which was prevented by inhibition of complement-mediated pathways in these mice[115]. As predominantly inactive synaptic connections were phagocytosed by microglia, the authors claim that the process is a physiological mechanism to delete and forget unimportant memories. In our study, the knockout of the CD11b gene (a subunit of complement receptor 3) partly prevented the phagocytosis of synapses following sepsis, suggesting that the same mechanism is also present in neuroinflammation. However, as the functional outcome for cognitive function was improved in knockout mice compared to wildtype mice, during sepsis it is rather a detrimental process due to an overreactive immune system. This has also been shown in Alzheimer models [73]. Hong et al. demonstrated that in early AD mouse models the complement pathway (e.g. C1q, C3) was upregulated and that synapses were phagocytosed by microglia in a complement-mediated process as inhibition of the complement pathway lowers the number of synapses

engulfed by microglia [73]. These findings also indicate that different causes (e.g. sepsis, neurodegenerative diseases) could induce an overreactive immune system in the brain which leads to complement-dependent microglia-mediated synapse loss. Interestingly, dopamine has been found to inhibit cytokine production and inflammation in the body following sepsis [116]. Furthermore, Li et al. report that L-Dopa/Benserazide, a dopamine decarboxylase inhibitor, therapy prevents long-term cognitive impairment in rodents [117]. This further suggests, that in sepsis-induced long-term cognitive deficits an overactive immune system is involved. Therefore, anti-inflammatory therapy might be a successful therapeutic strategy to prevent sepsis-induced long-term memory deficits.

5.3 Reduced synapse loss in phagocytic deficient mice

The maintenance of neuronal circuits is a delicate equilibrium of maturation and removal of synaptic components. During neuroinflammation, the balance is disrupted due to release of reactive oxygen species (ROS) by microglia [118]. ROS damage neurons and induce reversible externalization of PS which is recognized by microglia via different receptors [55-57]. PS externalization of cells leads to engulfment and phagocytosis, but it has been shown that *in vitro* phagocytosis can be prevented by blocking different receptors and ligands of microglia after cerebral ischemia [55]. Corresponding to our findings, Sheppard et al. were able to find evidence in organotypic hippocampal slice cultures (OHSCs) that LPS-induced synapse loss is mediated by microglia as it is prevented by depleting microglia before LPS application [119]. In our study, we observed a significant decrease in synapse number and correspondingly an increase in phagocytosis after i.p. LPS-injections *in vivo*, which is partly prevented in phagocytic deficient mice, suggesting that the *in vitro* - observed mechanism also applies *in vivo*.

However, as the phagocytosis is not completely prevented by knockout of a single protein, phagocytosis of synapses may be activated via different molecular pathways, that are at least partially redundant. It would be interesting to investigate whether knockout of several phagocytic proteins could

synergistically prevent phagocytosis even more efficiently and whether the functional outcome could also improve.

5.4 Phagocytosis of small apoptotic neuritic fragments by astrocytes

Just recently, Damisah et al. published their findings that both astrocytes and microglia are involved in phagocytosis of dying or dead neurons [120]. Whereas microglia were found to mainly phagocytose somata of neurons, astrocytes phagocytose apoptotic debris from the dendritic arbors. Thus, as not only microglia are responsible for removal of dead or dying neurons, incomplete prevention of phagocytosis by knockout of *Cd11b* or *Mfge8* might also be the consequence of still functional astrocytic phagocytosis. As *Mfge8* is expressed in astrocytes and microglia, but *Cd11b* only in microglia, the differences in both groups could reflect the involvement of astrocytes in sepsis-induced phagocytosis of dying neurons. Of note, Damisah et al. showed that microglial-specific knockout of *Mertk* delays the approach of microglia to the somata of dying neurons and that astrocytes compensate for the deficiency by phagocytosing also dead cell bodies. Therefore, it is possible that knockout of *Mfge8* or *Cd11b* also leads to a compensatory increase in astrocytic phagocytosis and that inhibition of microglial phagocytosis is insufficient for preventing sepsis-induced cognitive impairments.

5.5 Inhibition of phagocytosis might be a therapeutic strategy to prevent sepsis-induced long-term cognitive impairments

A specific therapeutic strategy to prevent cognitive deficits after sepsis is still missing. The current approach for improving the outcome after sepsis is to minimize the elapsed time until diagnosis and antibiotic treatment. However, the worse prognosis for elderly people suffering from sepsis shows that even early

antibiotic therapy is insufficient in preventing loss of independence for survivors. Our study, and the behavioral testing performed by our collaborators, indicates that the lack of single phagocytic proteins prevents inappropriate synaptic pruning and improves long-term cognitive function after sepsis. Interestingly, our collaborating group in Berlin also tested cognitive functions in wildtype mice treated with cilengitide, a cyclic RGD pentapeptide inhibiting integrins αvβ3, αvβ5 and αvβ1. [121] As explained in section *2.3.1.1.1* MFG-E8 bridges apoptotic cells and phagocytes via binding to phosphatidyl serine and the vitronectin receptor, which consists of αvβ3/5 integrin subunits. [56] By blocking the vitronectin receptor, cilengitide is able to prevent the interaction between apoptotic cells, MFG-E8 and phagocytes (*Figure 3)* and might therefore be a potential drug to preserve cognitive functions after sepsis. However, it is currently researched as a potential oncological drug for glioblastoma therapy. [121]

Using cilengitide, Mei et al. were able to show that pharmacological inhibition of the vitronectin receptor prevents sepsis-induced cognitive impairments in rodents. In the future, a possible inhibition of these proteins might be an interesting approach to specifically prevent sepsis-induced cognitive impairment. As analyses in wildtype animals show however, most synapses are phagocytosed within one or two days. Sheppard et al. were able to demonstrate in OHSCs that depleting microglia 24h hours after LPS application does not prevent synapse loss compared to non-treated OHSCs [119]. To be able to prevent cognitive decline after sepsis, Mei et al. injected Cilengitide for 7 days directly after LPS-injections. Therefore, it is still questionable whether a pharmaceutical inhibition of microglial phagocytosis would be fast enough to prevent the acute reaction as identifying the onset and initiating the therapy of systemic inflammation is often delayed in clinical settings. Nevertheless, further research would reveal deeper insights into the mechanisms behind sepsis-induced impairment and new therapeutic strategies might be elicited.

5.6 Conclusion

In line with previous studies, the work presented here confirms that i.p. injected LPS leads to a general inflammation in the CNS as well as activation of microglia. Furthermore, acutely after LPS-treatment synapse loss and increase in phagocytosed synapses could be detected in cortex and CA1. Although biochemical and immunohistochemical parameters were normalized within a week, behavioral tests, executed by collaborators, showed that the rodents suffered from long-term cognitive impairments two months after LPS-injections.

In neurodegenerative diseases, studies suggest that microglial overreaction is leading to a vicious cycle of neuronal damage and increased production of debris. In this regard, sepsis-induced CNS inflammation might also induce a vicious cycle of microglial overreaction and synaptic pruning, causing reduced synaptic connections and impaired neuronal circuits. Although histologically synapse number is normalized after one week, the required amount of time is much larger for re-establishing neuronal circuits than for dendritic spine sprouting. This might explain the evidence for cognitive impairments two months after LPS-injections in behavioral tests without immunohistochemical indications.

The inability to prevent synaptic pruning in phagocytosis deficient mice demonstrate that the pathophysiology behind sepsis-induced cognitive impairment is complex and mediated by different mechanisms. New findings suggest that several proteins are involved in this process and also that not only microglia but also astrocytes are important for neuronal phagocytosis. This might be the reason why one single protein knockout did not completely prevent synapse loss. Therefore, further research is necessary and important to be able to depict the role of different cell types, proteins and pathways in sepsis-induced cognitive impairments. Further insights in the cellular processes underlying sepsis-induced cognitive decline might also reveal new therapeutic strategies to treat sepsis-induced cognitive impairments more efficiently than by antibiotic therapy alone.

6 German Summary

Die Sepsis ist eine schwerwiegende Erkrankung, die auch heutzutage mit einer Mortalität von 30-50% eine gefürchtete Komplikation auf Intensivstationen ist. Epidemiologische Untersuchungen haben ergeben, dass von den circa 400 000 Patienten pro Jahr, die an einer Sepsis erkranken, vor allem Kleinkinder unter einem Jahr sowie ältere Menschen über 65 Jahre betroffen sind. Mit dem demografischen Wandel und den zunehmenden Erfolgen der Intensivmedizin stellt die Sepsis daher eine erhebliche Mehrbelastung für das Gesundheitssystem dar. Bei 60% der Überlebenden können auch lange Zeit nach der akuten Erkrankung kognitive Defizite festgestellt werden, die zu einer erhöhten Rate an Pflegebedürftigkeit und Lebensqualitätsverlust und damit zu nicht unerheblichen Kosten für das Gesundheitssystem führt.

Trotz der großen Relevanz für das Gesundheitssystem sind die Ursachen und die Pathophysiologie der kognitiven Einschränkung nach einer Sepsis nicht hinreichend untersucht. Verschiedene Studien suggerieren einen Zusammenhang zwischen den gehirneigenen Makrophagen, den Mikroglia, und den kognitiven Verlusten nach peripherer Inflammation.

Mikroglia repräsentieren 10-15% der Zellen im Gehirn und haben vielfältige Aufgaben im Zentralen Nervensystem. Sie erhalten z.Bsp. die Homeostase im Gehirn, indem sie alte Neurone und vermeintlich toxische extrazellulären Komponenten phagozytieren. Vor allem während dem Heranwachsen und Ausbilden der neuronalen Netzwerke im Gehirn spielen Mikroglia eine entscheidende Rolle. In einem durch das Komplementsystem gesteuerten Vorgang phagozytieren Mikroglia inaktive Synapsen und helfen dabei der Ausbildung von nützlichen Verknüpfungen im Gehirn. Für die Phagozytose wichtige Proteine sind vor allem Mer receptor tyrosine kinase (Mertk), milk fat globule EGF-like factor 8 (MFG-E8) und cluster of differentiation molecule 11b (CD11b) bekannt.

Um die Pathophysiologie von kognitiven Einschränkungen nach einer Sepsis besser zu verstehen, wurden hier in verschiedenen Mausmodellen jeweils Wildtyp- und homozygote Knockout-Tiere *(Mfge8, Cd11b, Mertk)* durch eine intraperitonealen (i.p.) Injektion von Lipopolysacchariden (LPS) Injektion eine periphere Inflammation ausgelöst. Die Tiere wurden nach 1 Tag, 3 Tage, 7 Tagen oder 2 Monaten euthanasiert und die Gehirnproben mittels Immunhistologie oder biochemischen Analysen untersucht.

Die biochemische Untersuchung des Komplementproteins 3 (C3) ergab in allen Genotypen eine akute Verdoppelung der Konzentration des Proteins im Gehirn. Untersuchungen an Gewebeschnitten der behandelten Tiere zeigten eine über 3 Tage anhaltende Vergrößerung der Mikroglia und zudem eine leichte Vergrößerung des Gehirnvolumens bzw. Ventrikelvolumens. Diese Beobachtungen weisen auf eine akute Inflammation nach Sepsis hin.

In Gehirnhomogenaten wurde außerdem die Erhöhung einiger proinflammatorischen Zytokine in *Cd11b* Knockout-Tiere zwei Monate nach LPS Injektion gefunden. Dieser Effekt könnte jedoch am fehlenden suppressiven Einfluss von CD11b auf das Immunsystem liegen.

Vor allem in *Mfge8* Wildtyp-Tieren konnte mittels Immunhistologie ein gravierender Verlust an funktionalen Synapsen im Cortex und im Hippocampus dargestellt werden. Außerdem wurde in *Cd11b* und *Mfge8* Wildtyp-Mäusen eine vermehrte Phagozytose von Synapsen 1 bis 3 Tage nach der LPS Injektion festgestellt. Der Synapsenverlust zusammen mit der vermehrten Phagozytose konnte in den korrespondierenden knockout Tieren verhindert werden, sodass zum ersten Mal ein Hinweis gefunden wurde, dass vor allem MFG-E8 eine Rolle in der Phagozytose von Synapsen nach einer Sepsis spielt.

Zusammenfassend zeigen die biochemischen und immunhistologischen Untersuchungen eine Überaktivierung von Mikroglia nach LPS-injektionen, die zu einem akuten, ausgeprägten Synapsenverlust nach Sepsis führt. Die Inhibition der Phagozytose durch genetische Knockouts von beteiligten Proteinen verhindert teilweise diesen Verlust. Die Kollaborationspartner in Berlin (AG

Emmrich) fanden in verschiedenen Verhaltenstest eine deutliche Einschränkung des räumlichen und emotionalen Gedächtnisses der Tiere nach LPS Injektionen, welche teilweise durch den Knockout der Phagozytose-assoziierten Proteine verhindert werden konnte.

Diese Erkenntnisse, zusammen mit den biochemischen und immunhistochemischen Ergebnissen sind ein erster Hinweis, dass mikrogliale Phagozytose ein wichtiger Pathomechanismus für kognitive Einschränkungen nach einer Sepsis sein könnte.

7 Reference list

1. Pandharipande PP, Girard TD, Ely EW. Long-term cognitive impairment after critical illness. N Engl J Med. 2014;370(2):185-186.
2. Ehlenbach WJ, Hough CL, Crane PK, et al. Association between acute care and critical illness hospitalization and cognitive function in older adults. JAMA. 2010;303(8):763-770.
3. Kreymann G, Wolf M. [History and definition of sepsis--do we need new terminology?]. Anasthesiol Intensivmed Notfallmed Schmerzther. 1996;31(1):9-14.
4. Sykes R. Penicillin: from discovery to product. Bull World Health Organ. 2001;79(8):778-779.
5. Deutschman CS, Tracey KJ. Sepsis: current dogma and new perspectives. Immunity. 2014;40(4):463-475.
6. American College of Chest Physicians/Society of Critical Care Medicine Consensus Conference: definitions for sepsis and organ failure and guidelines for the use of innovative therapies in sepsis. Crit Care Med. 1992;20(6):864-874.
7. Levy MM, Fink MP, Marshall JC, et al. 2001 SCCM/ESICM/ACCP/ATS/SIS International Sepsis Definitions Conference. Crit Care Med. 2003;31(4):1250-1256.
8. Singer M, Deutschman CS, Seymour CW, et al. The Third International Consensus Definitions for Sepsis and Septic Shock (Sepsis-3). JAMA. 2016;315(8):801-810.
9. Mak MHW, Low JK, Junnarkar SP, et al. A prospective validation of Sepsis-3 guidelines in acute hepatobiliary sepsis: qSOFA lacks sensitivity and SIRS criteria lacks specificity (Cohort Study). Int J Surg. 2019;72:71-77.
10. Huggan PJ, Bell A, Waetford J, et al. Evidence of High Mortality and Increasing Burden of Sepsis in a Regional Sample of the New Zealand Population. Open Forum Infect Dis. 2017;4(3):ofx106.
11. Fleischmann C, Scherag A, Adhikari NK, et al. Assessment of Global Incidence and Mortality of Hospital-treated Sepsis. Current Estimates and Limitations. Am J Respir Crit Care Med. 2016;193(3):259-272.
12. Fleischmann C, Thomas-Rueddel DO, Hartmann M, et al. Hospital Incidence and Mortality Rates of Sepsis. Dtsch Arztebl Int. 2016;113(10):159-166.
13. Langa KM, Chernew ME, Kabeto MUcoIsahbaaIactapbcgAdschidad, et al. National estimates of the quantity and cost of informal caregiving for the elderly with dementia. J Gen Intern Med. 2001;16(11):770-778.
14. van Beusekom I, Bakhshi-Raiez F, de Keizer NF, et al. Healthcare costs of ICU survivors are higher before and after ICU admission compared to a population based control group: A descriptive study combining healthcare insurance data and data from a Dutch national quality registry. J Crit Care. 2018;44:345-351.
15. Arefian H, Heublein S, Scherag A, et al. Hospital-related cost of sepsis: A systematic review. J Infect. 2017;74(2):107-117.

16. Angus DC, Linde-Zwirble WT, Lidicker J, et al. Epidemiology of severe sepsis in the United States: analysis of incidence, outcome, and associated costs of care. Crit Care Med. 2001;29(7):1303-1310.
17. Paoli CJ, Reynolds MA, Sinha M, et al. Epidemiology and Costs of Sepsis in the United States-An Analysis Based on Timing of Diagnosis and Severity Level. Crit Care Med. 2018;46(12):1889-1897.
18. Herridge MS, Cheung AM, Tansey CM, et al. One-year outcomes in survivors of the acute respiratory distress syndrome. N Engl J Med. 2003;348(8):683-693.
19. Schmid A, Burchardi H, Clouth J, et al. Burden of illness imposed by severe sepsis in Germany. Eur J Health Econ. 2002;3(2):77-82.
20. Sprung CL, Peduzzi PN, Shatney CH, et al. Impact of encephalopathy on mortality in the sepsis syndrome. The Veterans Administration Systemic Sepsis Cooperative Study Group. Crit Care Med. 1990;18(8):801-806.
21. Iacobone E, Bailly-Salin J, Polito A, et al. Sepsis-associated encephalopathy and its differential diagnosis. Crit Care Med. 2009;37(10 Suppl):S331-336.
22. Pandharipande PP, Girard TD, Jackson JC, et al. Long-term cognitive impairment after critical illness. N Engl J Med. 2013;369(14):1306-1316.
23. Torgersen J, Hole JF, Kvale R, et al. Cognitive impairments after critical illness. Acta Anaesthesiol Scand. 2011;55(9):1044-1051.
24. Jackson JC, Hart RP, Gordon SM, et al. Six-month neuropsychological outcome of medical intensive care unit patients. Crit Care Med. 2003;31(4):1226-1234.
25. Aguero-Torres H, von Strauss E, Viitanen M, et al. Institutionalization in the elderly: the role of chronic diseases and dementia. Cross-sectional and longitudinal data from a population-based study. J Clin Epidemiol. 2001;54(8):795-801.
26. Polito A, Eischwald F, Maho AL, et al. Pattern of brain injury in the acute setting of human septic shock. Crit Care. 2013;17(5):R204.
27. Semmler A, Widmann CN, Okulla T, et al. Persistent cognitive impairment, hippocampal atrophy and EEG changes in sepsis survivors. J Neurol Neurosurg Psychiatry. 2013;84(1):62-69.
28. Morandi A, Rogers BP, Gunther ML, et al. The relationship between delirium duration, white matter integrity, and cognitive impairment in intensive care unit survivors as determined by diffusion tensor imaging: the VISIONS prospective cohort magnetic resonance imaging study*. Crit Care Med. 2012;40(7):2182-2189.
29. Sharshar T, Annane D, de la Grandmaison GL, et al. The neuropathology of septic shock. Brain Pathol. 2004;14(1):21-33.
30. Lemstra AW, Groen in't Woud JC, Hoozemans JJ, et al. Microglia activation in sepsis: a case-control study. J Neuroinflammation. 2007;4:4.
31. Jakel S, Dimou L. Glial Cells and Their Function in the Adult Brain: A Journey through the History of Their Ablation. Front Cell Neurosci. 2017;11:24.
32. Kimelberg HK. Functions of mature mammalian astrocytes: a current view. Neuroscientist. 2010;16(1):79-106.
33. Askew K, Li K, Olmos-Alonso A, et al. Coupled Proliferation and Apoptosis Maintain the Rapid Turnover of Microglia in the Adult Brain. Cell Rep. 2017;18(2):391-405.

34. Ajami B, Bennett JL, Krieger C, et al. Local self-renewal can sustain CNS microglia maintenance and function throughout adult life. Nat Neurosci. 2007;10(12):1538-1543.
35. Kreutzberg GW. Microglia, the first line of defence in brain pathologies. Arzneimittelforschung. 1995;45(3A):357-360.
36. Lawson LJ, Perry VH, Gordon S. Turnover of resident microglia in the normal adult mouse brain. Neuroscience. 1992;48(2):405-415.
37. Brown GC, Neher JJ. Microglial phagocytosis of live neurons. Nat Rev Neurosci. 2014;15(4):209-216.
38. Dheen ST, Kaur C, Ling EA. Microglial activation and its implications in the brain diseases. Curr Med Chem. 2007;14(11):1189-1197.
39. Arienti S, Barth ND, Dorward DA, et al. Regulation of Apoptotic Cell Clearance During Resolution of Inflammation. Front Pharmacol. 2019;10:891.
40. Abdolmaleki F, Farahani N, Gheibi Hayat SM, et al. The Role of Efferocytosis in Autoimmune Diseases. Front Immunol. 2018;9:1645.
41. Peng Y, Elkon KB. Autoimmunity in MFG-E8-deficient mice is associated with altered trafficking and enhanced cross-presentation of apoptotic cell antigens. J Clin Invest. 2011;121(6):2221-2241.
42. Cohen PL, Caricchio R, Abraham V, et al. Delayed apoptotic cell clearance and lupus-like autoimmunity in mice lacking the c-mer membrane tyrosine kinase. J Exp Med. 2002;196(1):135-140.
43. Hill RA, Li AM, Grutzendler J. Lifelong cortical myelin plasticity and age-related degeneration in the live mammalian brain. Nat Neurosci. 2018;21(5):683-695.
44. Safaiyan S, Kannaiyan N, Snaidero N, et al. Age-related myelin degradation burdens the clearance function of microglia during aging. Nat Neurosci. 2016;19(8):995-998.
45. Sikorska K, Gradzka I, Sochanowicz B, et al. Diminished amyloid-beta uptake by mouse microglia upon treatment with quantum dots, silver or cerium oxide nanoparticles: Nanoparticles and amyloid-beta uptake by microglia. Hum Exp Toxicol. 2019:960327119880586.
46. Efthymiou AG, Goate AM. Late onset Alzheimer's disease genetics implicates microglial pathways in disease risk. Mol Neurodegener. 2017;12(1):43.
47. Villegas-Llerena C, Phillips A, Garcia-Reitboeck P, et al. Microglial genes regulating neuroinflammation in the progression of Alzheimer's disease. Curr Opin Neurobiol. 2016;36:74-81.
48. Mawuenyega KG, Sigurdson W, Ovod V, et al. Decreased clearance of CNS beta-amyloid in Alzheimer's disease. Science. 2010;330(6012):1774.
49. Ciesielski-Treska J, Grant NJ, Ulrich G, et al. Fibrillar prion peptide (106-126) and scrapie prion protein hamper phagocytosis in microglia. Glia. 2004;46(2):101-115.
50. Janda E, Boi L, Carta AR. Microglial Phagocytosis and Its Regulation: A Therapeutic Target in Parkinson's Disease? Front Mol Neurosci. 2018;11:144.
51. Galloway DA, Phillips AEM, Owen DRJ, et al. Phagocytosis in the Brain: Homeostasis and Disease. Front Immunol. 2019;10:790.
52. Gleiss B, Gogvadze V, Orrenius S, et al. Fas-triggered phosphatidylserine exposure is modulated by intracellular ATP. FEBS Lett. 2002;519(1-3):153-158.

53. Tyurina YY, Basova LV, Konduru NV, et al. Nitrosative stress inhibits the aminophospholipid translocase resulting in phosphatidylserine externalization and macrophage engulfment: implications for the resolution of inflammation. J Biol Chem. 2007;282(11):8498-8509.
54. Weiss E, Cytlak UM, Rees DC, et al. Deoxygenation-induced and Ca(2+) dependent phosphatidylserine externalisation in red blood cells from normal individuals and sickle cell patients. Cell Calcium. 2012;51(1):51-56.
55. Neher JJ, Neniskyte U, Zhao JW, et al. Inhibition of microglial phagocytosis is sufficient to prevent inflammatory neuronal death. J Immunol. 2011;186(8):4973-4983.
56. Fricker M, Neher JJ, Zhao JW, et al. MFG-E8 mediates primary phagocytosis of viable neurons during neuroinflammation. J Neurosci. 2012;32(8):2657-2666.
57. Neher JJ, Emmrich JV, Fricker M, et al. Phagocytosis executes delayed neuronal death after focal brain ischemia. Proc Natl Acad Sci U S A. 2013;110(43):E4098-4107.
58. Miyanishi M, Tada K, Koike M, et al. Identification of Tim4 as a phosphatidylserine receptor. Nature. 2007;450(7168):435-439.
59. Kobayashi N, Karisola P, Pena-Cruz V, et al. TIM-1 and TIM-4 glycoproteins bind phosphatidylserine and mediate uptake of apoptotic cells. Immunity. 2007;27(6):927-940.
60. Hanayama R, Tanaka M, Miwa K, et al. Identification of a factor that links apoptotic cells to phagocytes. Nature. 2002;417(6885):182-187.
61. Matsuda A, Jacob A, Wu R, et al. Milk fat globule-EGF factor VIII in sepsis and ischemia-reperfusion injury. Mol Med. 2011;17(1-2):126-133.
62. Bu HF, Zuo XL, Wang X, et al. Milk fat globule-EGF factor 8/lactadherin plays a crucial role in maintenance and repair of murine intestinal epithelium. J Clin Invest. 2007;117(12):3673-3683.
63. Silvestre JS, Thery C, Hamard G, et al. Lactadherin promotes VEGF-dependent neovascularization. Nat Med. 2005;11(5):499-506.
64. Hornik TC, Vilalta A, Brown GC. Activated microglia cause reversible apoptosis of pheochromocytoma cells, inducing their cell death by phagocytosis. J Cell Sci. 2016;129(1):65-79.
65. Lemke G, Rothlin CV. Immunobiology of the TAM receptors. Nat Rev Immunol. 2008;8(5):327-336.
66. Shao WH, Zhen Y, Eisenberg RA, et al. The Mer receptor tyrosine kinase is expressed on discrete macrophage subpopulations and mainly uses Gas6 as its ligand for uptake of apoptotic cells. Clin Immunol. 2009;133(1):138-144.
67. Scott RS, McMahon EJ, Pop SM, et al. Phagocytosis and clearance of apoptotic cells is mediated by MER. Nature. 2001;411(6834):207-211.
68. Matsumoto Y, Watabe K, Ikuta F. Immunohistochemical study on neuroglia identified by the monoclonal antibody against a macrophage differentiation antigen (Mac-1). J Neuroimmunol. 1985;9(6):379-389.
69. Khan SQ, Khan I, Gupta V. CD11b Activity Modulates Pathogenesis of Lupus Nephritis. Front Med (Lausanne). 2018;5:52.
70. Springer T, Galfre G, Secher DS, et al. Mac-1: a macrophage differentiation antigen identified by monoclonal antibody. Eur J Immunol. 1979;9(4):301-306.

71. Fagerholm SC, Varis M, Stefanidakis M, et al. alpha-Chain phosphorylation of the human leukocyte CD11b/CD18 (Mac-1) integrin is pivotal for integrin activation to bind ICAMs and leukocyte extravasation. Blood. 2006;108(10):3379-3386.
72. Bodea LG, Wang Y, Linnartz-Gerlach B, et al. Neurodegeneration by activation of the microglial complement-phagosome pathway. J Neurosci. 2014;34(25):8546-8556.
73. Hong S, Beja-Glasser VF, Nfonoyim BM, et al. Complement and microglia mediate early synapse loss in Alzheimer mouse models. Science. 2016;352(6286):712-716.
74. Schafer DP, Lehrman EK, Kautzman AG, et al. Microglia sculpt postnatal neural circuits in an activity and complement-dependent manner. Neuron. 2012;74(4):691-705.
75. Berg A, Zelano J, Stephan A, et al. Reduced removal of synaptic terminals from axotomized spinal motoneurons in the absence of complement C3. Exp Neurol. 2012;237(1):8-17.
76. Stevens B, Allen NJ, Vazquez LE, et al. The classical complement cascade mediates CNS synapse elimination. Cell. 2007;131(6):1164-1178.
77. Neniskyte U, Neher JJ, Brown GC. Neuronal death induced by nanomolar amyloid beta is mediated by primary phagocytosis of neurons by microglia. J Biol Chem. 2011;286(46):39904-39913.
78. Driessen RGH, van de Poll MCG, Mol MF, et al. The influence of a change in septic shock definitions on intensive care epidemiology and outcome: comparison of sepsis-2 and sepsis-3 definitions. Infect Dis (Lond). 2018;50(3):207-213.
79. Buras JA, Holzmann B, Sitkovsky M. Animal models of sepsis: setting the stage. Nat Rev Drug Discov. 2005;4(10):854-865.
80. Dantzer R, O'Connor JC, Freund GG, et al. From inflammation to sickness and depression: when the immune system subjugates the brain. Nat Rev Neurosci. 2008;9(1):46-56.
81. Bluthe RM, Walter V, Parnet P, et al. Lipopolysaccharide induces sickness behaviour in rats by a vagal mediated mechanism. C R Acad Sci III. 1994;317(6):499-503.
82. Biesmans S, Meert TF, Bouwknecht JA, et al. Systemic immune activation leads to neuroinflammation and sickness behavior in mice. Mediators Inflamm. 2013;2013:271359.
83. Qin L, Wu X, Block ML, et al. Systemic LPS causes chronic neuroinflammation and progressive neurodegeneration. Glia. 2007;55(5):453-462.
84. Anderson ST, Commins S, Moynagh PN, et al. Lipopolysaccharide-induced sepsis induces long-lasting affective changes in the mouse. Brain Behav Immun. 2015;43:98-109.
85. Semmler A, Frisch C, Debeir T, et al. Long-term cognitive impairment, neuronal loss and reduced cortical cholinergic innervation after recovery from sepsis in a rodent model. Exp Neurol. 2007;204(2):733-740.
86. Semmler A, Okulla T, Sastre M, et al. Systemic inflammation induces apoptosis with variable vulnerability of different brain regions. J Chem Neuroanat. 2005;30(2-3):144-157.

87. Coxon A, Rieu P, Barkalow FJ, et al. A novel role for the beta 2 integrin CD11b/CD18 in neutrophil apoptosis: a homeostatic mechanism in inflammation. Immunity. 1996;5(6):653-666.
88. Lu Q, Gore M, Zhang Q, et al. Tyro-3 family receptors are essential regulators of mammalian spermatogenesis. Nature. 1999;398(6729):723-728.
89. Mei J. Sepsis-associated cognitive dysfunction: an investigation using stress-free, automated behavioral tests Available: http://dx.doi.org/10.17169/refubium-27183. Accessed 6th July, 2020.
90. Ippolito DM, Eroglu C. Quantifying synapses: an immunocytochemistry-based assay to quantify synapse number. J Vis Exp. 2010(45).
91. Morrison DC, Kline LF. Activation of the classical and properdin pathways of complement by bacterial lipopolysaccharides (LPS). J Immunol. 1977;118(1):362-368.
92. Papadopoulos MC, Lamb FJ, Moss RF, et al. Faecal peritonitis causes oedema and neuronal injury in pig cerebral cortex. Clin Sci (Lond). 1999;96(5):461-466.
93. Ari I, Kafa IM, Kurt MA. Perimicrovascular edema in the frontal cortex in a rat model of intraperitoneal sepsis. Exp Neurol. 2006;198(1):242-249.
94. Karimy JK, Zhang J, Kurland DB, et al. Inflammation-dependent cerebrospinal fluid hypersecretion by the choroid plexus epithelium in posthemorrhagic hydrocephalus. Nat Med. 2017;23(8):997-1003.
95. Han C, Jin J, Xu S, et al. Integrin CD11b negatively regulates TLR-triggered inflammatory responses by activating Syk and promoting degradation of MyD88 and TRIF via Cbl-b. Nat Immunol. 2010;11(8):734-742.
96. Deacon RM. Assessing nest building in mice. Nat Protoc. 2006;1(3):1117-1119.
97. Dantzer R. Cytokine, sickness behavior, and depression. Neurol Clin. 2006;24(3):441-460.
98. Granger JI, Ratti PL, Datta SC, et al. Sepsis-induced morbidity in mice: effects on body temperature, body weight, cage activity, social behavior and cytokines in brain. Psychoneuroendocrinology. 2013;38(7):1047-1057.
99. Konsman JP, Veeneman J, Combe C, et al. Central nervous action of interleukin-1 mediates activation of limbic structures and behavioural depression in response to peripheral administration of bacterial lipopolysaccharide. Eur J Neurosci. 2008;28(12):2499-2510.
100. Almeida MC, Steiner AA, Branco LG, et al. Cold-seeking behavior as a thermoregulatory strategy in systemic inflammation. Eur J Neurosci. 2006;23(12):3359-3367.
101. Spruijt BM, DeVisser L. Advanced behavioural screening: automated home cage ethology. Drug Discov Today Technol. 2006;3(2):231-237.
102. Goulding EH, Schenk AK, Juneja P, et al. A robust automated system elucidates mouse home cage behavioral structure. Proc Natl Acad Sci U S A. 2008;105(52):20575-20582.
103. Galsworthy MJ, Amrein I, Kuptsov PA, et al. A comparison of wild-caught wood mice and bank voles in the Intellicage: assessing exploration, daily activity patterns and place learning paradigms. Behav Brain Res. 2005;157(2):211-217.
104. Henstridge CM, Tzioras M, Paolicelli RC. Glial Contribution to Excitatory and Inhibitory Synapse Loss in Neurodegeneration. Front Cell Neurosci. 2019;13:63.

105. Neumann H, Takahashi K. Essential role of the microglial triggering receptor expressed on myeloid cells-2 (TREM2) for central nervous tissue immune homeostasis. J Neuroimmunol. 2007;184(1-2):92-99.
106. Bruel-Jungerman E, Davis S, Laroche S. Brain plasticity mechanisms and memory: a party of four. Neuroscientist. 2007;13(5):492-505.
107. Jorgensen HS, Nakayama H, Raaschou HO, et al. Outcome and time course of recovery in stroke. Part I: Outcome. The Copenhagen Stroke Study. Arch Phys Med Rehabil. 1995;76(5):399-405.
108. Jorgensen HS, Nakayama H, Raaschou HO, et al. Outcome and time course of recovery in stroke. Part II: Time course of recovery. The Copenhagen Stroke Study. Arch Phys Med Rehabil. 1995;76(5):406-412.
109. Hsu CY, Norris JW, Hogan EL, et al. Pentoxifylline in acute nonhemorrhagic stroke. A randomized, placebo-controlled double-blind trial. Stroke. 1988;19(6):716-722.
110. Hasbani MJ, Underhill, S. M., De Erausquin, G., & Goldberg, M. P. . Synapse Loss and Regeneration: A Mechanism for Functional Decline and Recovery after Cerebral Ischemia? The Neuroscientist. 2000;6(2):110-119.
111. Iwashyna TJ, Ely EW, Smith DM, et al. Long-term cognitive impairment and functional disability among survivors of severe sepsis. JAMA. 2010;304(16):1787-1794.
112. Dilger RN, Johnson RW. Aging, microglial cell priming, and the discordant central inflammatory response to signals from the peripheral immune system. J Leukoc Biol. 2008;84(4):932-939.
113. Hefendehl JK, Neher JJ, Suhs RB, et al. Homeostatic and injury-induced microglia behavior in the aging brain. Aging Cell. 2014;13(1):60-69.
114. Streit WJ, Sammons NW, Kuhns AJ, et al. Dystrophic microglia in the aging human brain. Glia. 2004;45(2):208-212.
115. Wang C, Yue H, Hu Z, et al. Microglia mediate forgetting via complement-dependent synaptic elimination. Science. 2020;367(6478):688-694.
116. Torres-Rosas R, Yehia G, Pena G, et al. Dopamine mediates vagal modulation of the immune system by electroacupuncture. Nat Med. 2014;20(3):291-295.
117. Li F, Zhang B, Duan S, et al. Small dose of L-dopa/Benserazide Hydrochloride improved sepsis-induced neuroinflammation and long-term cognitive dysfunction in sepsis mice. Brain Res. 2020:146780.
118. Ding X, Zhang M, Gu R, et al. Activated microglia induce the production of reactive oxygen species and promote apoptosis of co-cultured retinal microvascular pericytes. Graefes Arch Clin Exp Ophthalmol. 2017;255(4):777-788.
119. Sheppard O, Coleman MP, Durrant CS. Lipopolysaccharide-induced neuroinflammation induces presynaptic disruption through a direct action on brain tissue involving microglia-derived interleukin 1 beta. J Neuroinflammation. 2019;16(1):106.
120. Damisah EC, Hill RA, Rai A, et al. Astrocytes and microglia play orchestrated roles and respect phagocytic territories during neuronal corpse removal in vivo. Sci Adv. 2020;6(26):eaba3239.

121. Mas-Moruno C, Rechenmacher F, Kessler H. Cilengitide: the first anti-angiogenic small molecule drug candidate design, synthesis and clinical evaluation. Anticancer Agents Med Chem. 2010;10(10):753-768.

8 Erklärung zum Eigenteil

Die Arbeit wurde am Hertie-Institut für klinische Hirnforschung unter Betreuung von Dr. Jonas Neher durchgeführt. Die Konzeption der Studie erfolgte durch Dr. Jonas Neher, Dr. Julius Emmrich, Charité Berlin und Prof. Dr. Michael Heneka, DZNE Bonn.

Die Tiere wurden in der Charité Berlin durch die Arbeitsgruppe Dr. Julius Emmrich aufgezogen, behandelt und euthanasiert. Die Perfusion und die Entnahme der Gehirne geschahen ebenfalls durch die AG Emmrich. Die Durchführung und Auswertung der Verhaltensstudien erfolgte durch Jie Mei, AG Emmrich, Charité Berlin.

Die Probenverarbeitung (Homogenisation, Sectioning) wurde von Maren Lösch, Ulrike Obermüller, Katleen Wild und mir durchgeführt. Die Probenvorbereitung, die Färbungen (PSD-95, IBA-1, Bassoon), das Imaging, sowie die C3- und MFG-E8-ELISA wurden von mir nach Einarbeitung durch Jessica Wagner, PhD, durchgeführt. Die Cresyl Violett Färbungen wurde von Maren Lösch durchgeführt. Die Probenvorbereitung, das Imaging und die Auswertung wurden von mir durchgeführt. Die Mesoscale Zytokin Messungen wurden von Lisa Häsler und Rawaa Al-Shaana durchgeführt, die Probenvorbereitung und die Auswertung der Messwerte erfolgten jedoch durch mich. Die statistische Auswertung erfolgte nach Anleitung ebenfalls durch mich. Ich versichere, die Dissertationsschrift selbständig verfasst zu haben und keine weiteren als die von mir angegebenen Quellen verwendet zu haben.

Tübingen, den

9 Acknowledgments

I would like to thank my supervisor Dr. Jonas Neher for offering me this great opportunity to get insights into experimental laboratory work. It was a great pleasure to work in his group. Many thanks to Jessica Wagner for her patience, support and for all her answers to my never-ending questions. I would like to thank all my colleagues from the DZNE, Tübingen and Hertie Institute for the warm and helpful environment, especially Dr. Angelos Skodras for supporting me with the microscope work and Maren Lösch, Katleen Wild and Ulrike Obermüller for their help in tissue preparation.

I am thankful to Dr. Julius Emmrich, Dr. Jie Mei and Paolo Rosellini Tognetti from the Charité Universitätsmedizin, Berlin and Dr. Michael T. Heneka and Tatsuya Manabe from the DZNE, Bonn for providing the mouse tissue, the behavioral analysis and for the good cooperation in this study.